การดูดซับกรดคาร์บอกซิลิกบนอัลคาไลไททาเนทนาโนทิวบ์และไททาเนทที่มีโครงสร้างเป็นชั้น

ADSORPTION OF CARBOXYLIC ACIDS ON ALKALI TITANATE NANOTUBES AND LAYERED TITANATES MICROCRYSTALS

ลภัสรดา บุญศิริวิกร
วามิณี นิรามิษ
วิรัญญา จันสถาพร

โครงงานพิเศษนี้เป็นส่วนหนึ่งของการศึกษาตามหลักสูตร
ปริญญาวิทยาศาสตรบัณฑิต (เคมีอุตสาหกรรม)
ภาควิชาเคมี คณะวิทยาศาสตร์
สถาบันเทคโนโลยีพระจอมเกล้าเจ้าคุณทหารลาดกระบัง
ปีการศึกษา 2558

ADSORPTION OF CARBOXYLIC ACIDS ON ALKALI TITANATE NANOTUBES AND LAYERED TITANATES MICROCRYSTALS

LAPHATRADA BOONSIRIWIKORN
WAMINEE NIRAMIT
WIRANYA CHANSATAPORN

A SPECIAL PROJECT SUBMITTED IN PARTIAL FULFILLMENT OF
THE REQUIREMENT FOR
THE DEGREE OF BACHELOR OF SCIENCE (INDUSTRIAL CHEMISTRY)
DEPARTMENT OF CHEMISTRY, FACULTY OF SCIENCE
KING MONGKUT'S INSTITUTE OF TECHNOLOGY LADKRABANG
ACADEMIC YEAR 2015

Title	Adsorption of Carboxylic Acids on Alkali Titanate Nanotubes and Layered Titanates Microcrystals			
Students	Miss Laphatrada	Boonsiriwikorn	Student ID	55050789
	Miss Waminee	Niramit	Student ID	55050801
	Miss Wiranya	Chansataporn	Student ID	55050806
Degree	Bachelor of Science (Industrial Chemistry)			
Department	Chemistry			
Faculty	Science			
University	King Mongkut's Institute of Technology Ladkrabang (KMITL)			
Academic Year	2015			
Advisor	Assoc. Prof. Dr. Tawan Sooknoi			
Co-advisor	Dr. Tosapol Maluangnont			

Faculty of Science, King Mongkut's Insitute of Technology Ladkrabang (KMITL), has approved this special project submitted in partial fulfillment of the requirement for the degrees of Bachelor of Science (Industrial Chemistry) in academic year 2015.

Committees	Signatures
Asst. Prof. Dr. Pesak Rungrojchaipon Chairperson	
Asst. Prof. Dr. Punnama Siriphannon Committee	
Assoc. Prof. Dr. Tawan Sooknoi Committee and Advisor	
Dr. Tosapol Maluangnont Committee and Co-advisor	

Title	Adsorption of Carboxylic Acids on Alkali Titanate Nanotubes and Layered Titanates Microcrystals			
Students	Miss Laphatrada	Boonsiriwikorn	Student ID	55050789
	Miss Waminee	Niramit	Student ID	55050801
	Miss Wiranya	Chansataporn	Student ID	55050806
Degree	Bachelor of Science (Industrial Chemistry)			
Department	Chemistry			
Faculty	Science			
University	King Mongkut's Institute of Technology Ladkrabang (KMITL)			
Academic Year	2015			
Advisor	Assoc. Prof. Dr. Tawan Sooknoi			
Co-advisor	Dr. Tosapol Maluangnont			

Abstract

Titanate nanotubes (TNTs) were synthesized by an alkali hydrothermal treatment from P25 TiO_2. The TNTs were either washed with HCl or washed with deionized water. After calcination at 300 °C for 2 h, the crystal structure of TNTs-washed with HCl has changed from lepidocrocite into anatase phase. On the other hand, TNTs-washed with deionized water preserved the lepidocrocite structure. Carboxylic acids were adsorbed (by refluxing at 60 °C for 36 h) on TNTs retaining the lepidocrocite structure and also on related structures, including lepidocrocite titanate microcrystals $K_{0.8}Zn_{0.4}Ti_{1.6}O_4$, "step-three" layered $Na_2Ti_3O_7$, layered Li_2TiO_3 and $K_2Ti_6O_{13}$ with the tunnel structure. ATR and TGA showed that the adsorption of heptanoic acid on the external and internal surfaces of Li_2TiO_3 is higher than that on other materials, suggesting the high basicity of Li_2TiO_3. It is found that the surface area of material does not affect the adsorption capacity of carboxylic acid. The adsorption of several carboxylic acids with different number of carbon atoms on TNTs was investigated by GC, TGA and ATR. TGA showed that TNTs can adsorb a larger amount of di-carboxylic acid (sebacic acid, $(HCOO)C_8H_{16}(COOH)$, 17.4%) than mono-carboxylic acid (decanoic acid, $C_9H_{19}COOH$, 7.3%). Moreover, TNTs can adsorb a larger amount of long chain carboxylic acid compared to short chain carboxylic acids (i.e., 16.8% for palmitic acid vs 12.8% for propanoic acid). PXRD indicated that the adsorption of carboxylic acids on TNTs does not expand of the interlayer spaces. This result is in contrast to the adsorption on lepidocrocite titanate microcrystals where a small expansion (0.1 nm) was observed.

Keywords : Swelling, Titanate Nanotubes, Lepidocrocite, Carboxylic Acids

ACKNOWLEDGEMENT

For the thesis completion, the authors would like to thank the project advisor and coadvisor, Assoc. Prof. Dr. Tawan Sooknoi and Dr. Tosapol Maluangnont respectively, for their suggestion and coaching. They are also grateful for the examination committees including Asst. Prof. Dr. Pesak Rungrojchaipon and Asst. Prof. Dr. Punnama Siriphannon for their valuable comments.

The workplace and public utility are supported by the Department of Chemistry, Faculty of Science, King Mongkut's Institute of Technology Ladkrabang. We would like to specifically thank Mr. Pornanan Arsa for the TGA data of pure palmitic acid and advice on data analysis; Miss Naraya Pechsawang, Miss Pattaraporn Keawmanee and Miss Pattaraporn Visedsri for the $K_{0.8}Zn_{0.4}Ti_{1.6}O_4$ microcrystals and for $Na_2Ti_3O_7$; Mr. Sarin Maneenun, Mr. Supan Aiemlaor and Miss Saowalak Koomtongdee for $K_2Ti_6O_{13}$. We would also like to thank the member of the catalytic chemistry research unit (CCR) for help and suggestion.

Finally, we would like to acknowledge our families for their supports, love and spirit.

Laphatrada Boonsiriwikorn
Waminee Niramit
Wiranya Chansataporn

TABLE OF CONTENTS

TABLE OF CONTENTS (Continued)

TABLE OF CONTENTS (Continued)

LIST OF TABLES

LIST OF FIGURES

CHAPTER 1
INTRODUCTION

1.1 Motivation

Nowadays, functional materials are of interest for various fields of applications such as wastewater treatment, alternative energy, and catalysis. One of the most important requirement is that these materials possess high surface area, such that the large adsorption capacity or the improved catalytic activities can be achieved. Usually, the synthesis of high surface area materials such as zeolites or metal organic frameworks (MOFs) employs expensive structure-directing agent (template). Yet, some materials can be synthesized by a relatively easy and less expensive reagents. One of such example is titanate nanotubes (TNTs) having tubular morphology.

Nanotubular materials are being considered in various applications because of their special electronic and mechanical properties, high photocatalytic activity, large specific surface area, and high pore volume [1]. For example, it has been reported [1] that TNTs have a relatively higher interfacial charge transfer rate and higher surface area compared with the spherical TiO_2 particles, such that the nanotubes exhibit better photocatalytic activity.

TNTs have a diameter approximately 8-10 nm, length approximately 50-200 nm and the high surface area of 380-400 m^2/g [2,3]. There are three methods known to synthesize TNTs [1,4,5]: electrochemical deposition with templates, anodic oxidation of titanium metal, and hydrothermal treatment of TiO_2 with alkali solution. Nanotubes synthesized by hydrothermal treatment have a much smaller size and higher surface area than those by the other two routes. Some parameters affecting the formation of TiO_2-based nanotubes via hydrothermal method includes phases and particle sizes of starting materials, types and concentrations of alkali solution, temperature and duration of hydrothermal treatment, acid washing and calcination.

TNTs have high cation-exchange ability that allows for large active catalyst loadings. Such behavior is due to the presence of negatively charged O^{2-} sites at the external surfaces and at the internal surfaces. These sites interact with Na^+ in the hydrothermal synthesis, forming sodium-containing TNTs. Cation exchange results in the replacement of Na^+ by other cationic species such as protons [6,7]. However, besides simple mineral acids, little is known about the chemical reactivity of the O^{2-} sites in TNTs with respect to other types of probe molecules. So, this project investigates the chemical reactivity of the active sites in TNTs with respect to several molecules including carboxylic acids of different chain length. We will also compare the activity of TNTs with microcrystals of alkali titanate of related structures.

1.2 Objective

1.2.1 To investigate the reactivity of O^{2-} site in TNTs and related structure toward carboxylic acids.

1.2.2 To compare the adsorption of carboxylic acids on various titanate materials.

1.3 Scopes of project

1.3.1 Synthesis of TNTs by a hydrothermal method.

1.3.2 Cation exchange of TNTs with selected monovalent cation.

1.3.3 Investigation on the reactivity of O^{2-} sites in TNTs and related structure by the reaction of carboxylic acids with different chain length.

1.3.4 Characterization of pristine and modified TNTs (and layered titanates) by X-ray diffraction (XRD), Thermogravimetric analysis (TGA), Raman spectroscopy, attenuated total reflection spectroscopy (ATR), BET surface area measurement, scanning electron microscopy (SEM).

1.4 Expected result

It is expected that a new chemistry of O^{2-} sites in TNTs can be discovered.

CHAPTER 2
THEORY AND LITERATURE REVIEWS

2.1 Titanate nanotubes (TNTs)

2.1.1 Structure and mechanism

Titanate nanotubes (TNTs) can be easily and cheaply synthesized by a hydrothermal method employing TiO_2 nanopowder (P25) as a substrate [1,8].

TNTs have tubular open-end as shown in Figure 2.1. They can be defined as long, hollow cylinders. The large specific surface area of TNTs (from 100 to 478 m^2/g) and pore volume (from 0.25 to 1.1 cm^3/g) provide more effective reaction sites for photocatalysis. The external diameter of the typical TNTs is about 5–15 nm with the wall thickness of 2–6 nm. The length can vary from several tens to several hundreds of nanometers as shown in Figure 2.2. Most of the multilayered walls are asymmetric with the number of layers varying from 3 to 5 and an inter-shell spacing of about 0.78 nm as shown in Figure 2.3 [5]. It is widely accepted that the formation mechanism of nanotubes follows the 3D $\longrightarrow$ 2D $\longrightarrow$ 1D model [4,9]. Chemical bonds in the starting 3D TiO_2 will break under hydrothermal reaction, in which 2D layered entities will be formed and then convert into 1D nanotubes through sheet folding mechanism. The exact crystal structure of TNTs is still under debate. The two most common candidates are lepidocrocite titanate and $Na_2Ti_3O_7$.

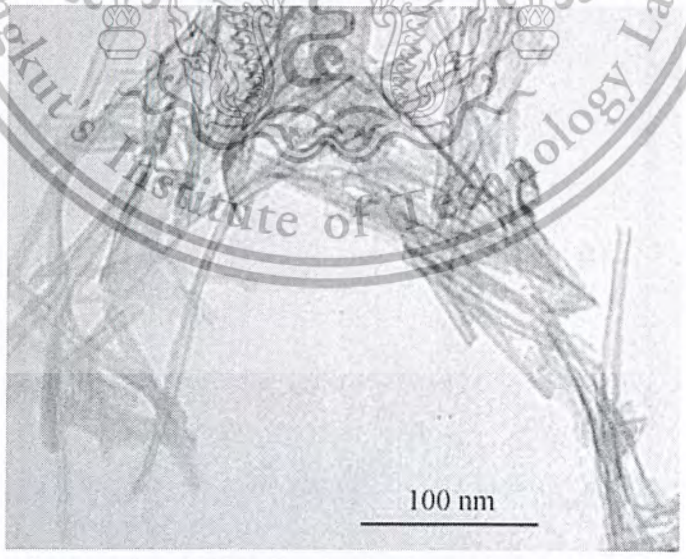

Figure 2.1 TEM micrographs of P25 after hydrothermal treatment in 10 mol/L NaOH solution at 160°C, 48 h, which shows that the nanotube is open-ended [10].

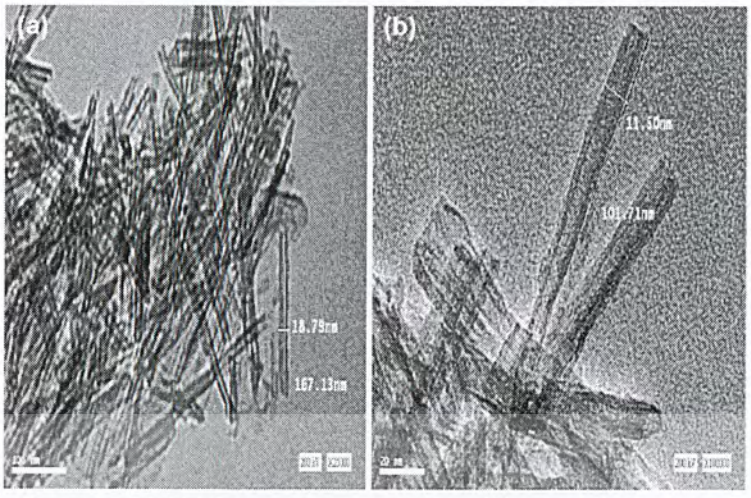

Figure 2.2 TEM for titania nanotube: (a) overall view and (b) detailed view of the tube structure [11].

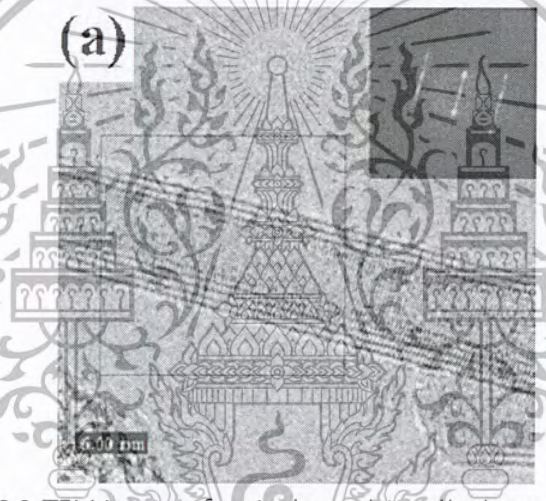

Figure 2.3 TEM image of a single multi-walled nanotube with an inter-shell spacing of 0.78 nm [5,12].

One mechanism for the formation of TNTs is the peeling-scrolling mechanism. This mechanism is deduced from the fact that nanosheets are observed in the early stage of formation from starting materials that are not tube-like. The breaking of Ti-O-Ti bonds and the subsequent formation of nanosheets are suggested [5]. Also, it is commonly observed that the total numbers of layers on the both sides of tubes are unequal, further suggesting that the sheets are curled up and form nanotubular structures. These TNTs consist of highly distorted TiO_6 octahedra. In general, the formation mechanism of TNTs during the hydrothermal process involves four stages [5]: (1) dissolution of TiO_2 precursor and breaking of Ti-O-Ti bonds in the concentrated alkaline solution; (2) formation and growth of layered titanate (whatever the exact structure is); (3) exfoliation of nanosheets; and (4) growing of nanosheets with the increasing tendency of curling.

2.1.2 Factors affecting TNTs synthesis by a hydrothermal method

Several factors can influence the formation of TNTs such as starting materials, types and concentrations of the alkali solution, hydrothermal temperature and duration and post-treatment processes (acid or deionized water washing and calcination). The main disadvantage of this nanotube fabrication method is the requirement of long reaction time in concentrated sodium hydroxide (NaOH) medium, which lead to the excessive intercalation of sodium ions in the produced nanotubes [13].

The hydrothermal process is more crucial in controlling nanotube formation than the post-treatment (acid washing procedure). It has been reported [14] that crystalline nanotubes could be formed prior to the acid or deionized water washing. That is, the acid treatment removes impurities [15,16] and also results in the formation of protonated titanates by ion exchange of Na^+ with H^+.

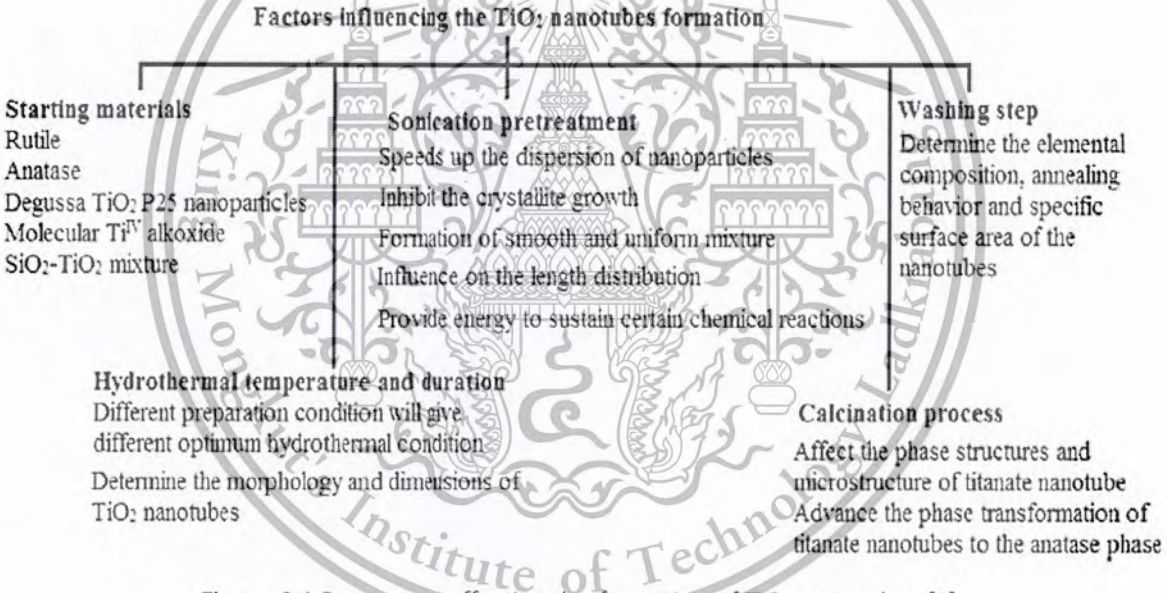

Figure 2.4 Parameters affecting the formation of TiO_2 nanotubes [1].

The effect of the starting materials has also been previously investigated. The use of P25 is known to produce TNTs several hundred nanometers in length and 7-15 nm in diameter [1]. The prepared nanotubes possessed uniform inner and outer diameters and they were multilayered and open-ended.

The type of alkali solution and their concentrations play an important role in the hydrothermal process. TNTs were generally prepared via hydrothermal treatment of TiO_2 powders in a 10 M NaOH solution. The high concentration of OH^- dissolves Ti^{4+} into the solution. The dissolved species in turn determines the rate of crystallization and the morphology of the final nanostructures [4].

The hydrothermal temperature is another essential factor in TNTs synthesis. The yield, length and degree of crystallinity of nanotubes increase with the hydrothermal temperature [17]. The optimal temperature exists in the range from 100°C to 200°C [18]. TNTs could be converted to nanofibers if the reaction time is too long. High yield of nanotubes having the surface area of 350 m^2/g could be synthesized when the NaOH concentration is adjusted to 10–15 M in the temperature range of 110–180°C with commercial P25 used as precursors [5].

Acid washing results in the ion-exchange process. When proton replaces sodium ions, the acid washed TNTs possess stronger hydroxyl bonds, a larger interlayer spacing, and an increase in specific surface area [4,19]. When washed TNTs with deionization water, only the external Na^+ ions are removed while the internal sodium cations remain within the structure.

The calcination process during post synthesis affects the crystal structure and microstructure of TNTs. Heat treatment transforms TNTs to the anatase phase via the elimination of sodium ions from the samples [1]. The H^+ loss in TNTs leads to a transformation in the sequence of $H_2Ti_3O_7{\cdot}xH_2O \longrightarrow H_2Ti_3O_7 \longrightarrow H_2Ti_6O_{13} \longrightarrow TiO_2(B) \longrightarrow TiO_2$ (anatase) when calcination temperature is in the range 140-500°C [20]. Nonetheless, the tubular structure collapses and the surface area decreases at the higher calcination temperature.

2.1.3 Reaction of TNTs

2.1.3.1 Ion exchange with acid

The Na^+ cations originally present in TNTs can be exchanged with protons during the washing step. It has been reported [21] that such ion exchange results in an increase in the specific surface area.

2.1.3.2 Ion exchange with other cations

TNTs show high ion-exchange reactivity with alkali metal cations. The cations might also enable better crystallinity of the nanotubes [22]. Cations reported to ion exchange into TNTs include H^+, Na^+ and Cs^+.

2.1.3.3 Metal or non-metal loading on TNTs

Various metal nanoparticles such as Pt, Au and Ag have been loaded onto TNTs [4]. Besides, the doping of TNTs with non-metal ions including N, S and C has been reported as well.

2.2 Related structure

2.2.1 Lepidocrocite titanate

Lepidocrocite titanates have the formula $A_xM_yTi_zO_4$. Here, A is an alkali metal, M is a transition metal having the valence not equal to +4, or the cation vacancy, and the subscripts x, y and z indicate appropriate stoichiometry. Lepidocrocite titanates have a layered structure comprising of $(Ti,M)O_6$ octahedra joining via the edges forming sheets. These sheets stack along the b-direction of the orthorhombic unit cell, with the alkali metal cations residing between the layers as shown in Figure 2.5. These titanates exhibit chemical reactivity typical for layered materials such as ion-exchange, intercalation, and swelling. Recent work in our group has shown that the repeating distance of 0.8 nm in Lepidocrocite titanates ($K_{0.8}Zn_{0.4}Ti_{1.6}O_4$) expanded to 1.2 nm due to the intercalation of palmitic acid, with the long molecular axis parallel to the sheets [23].

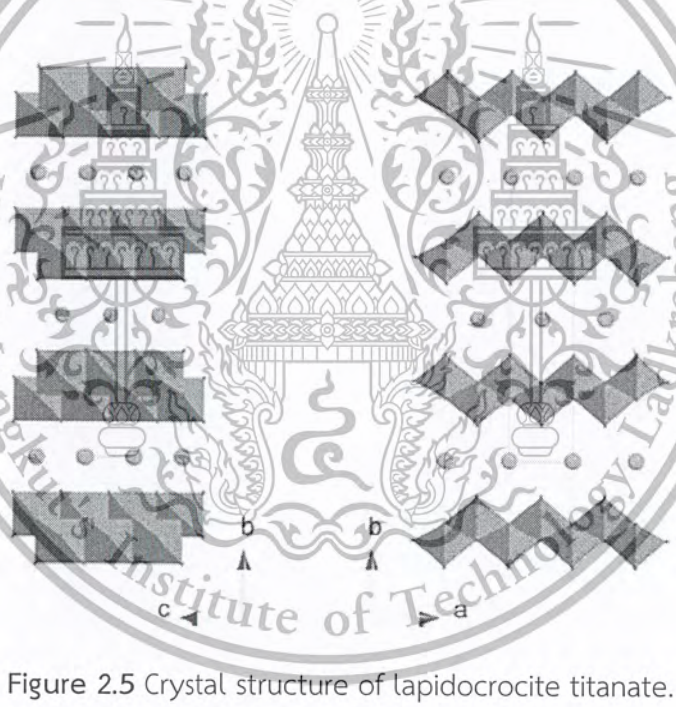

Figure 2.5 Crystal structure of lapidocrocite titanate.

2.2.2 $Na_2Ti_3O_7$

The sodium trititanate ($Na_2Ti_3O_7$) structure consists of zigzag layers of TiO_6 octahedra as shown in Figure 2.6. The Na^+ is located between the layers of TiO_6 and can be exchanged by other cations. The micro-structure of the $Na_2Ti_3O_7$ is nanotubes. The inside diameter of these nanotubes is about 4 nm, outside diameter is about 6 nm and the lengths are from 200 to 500 nm [24,25].

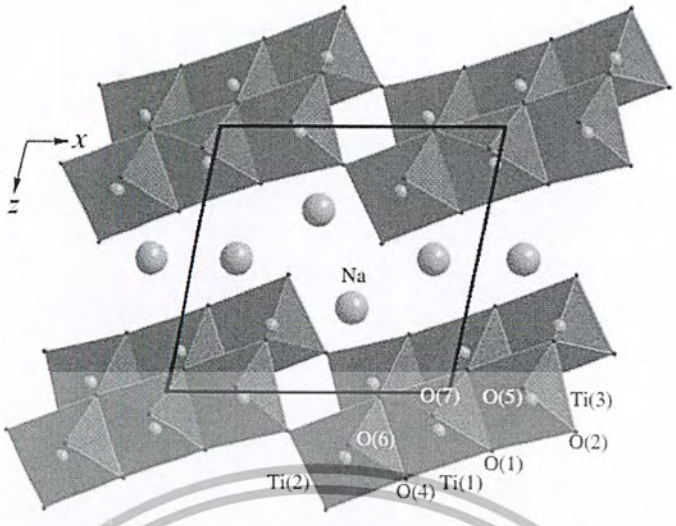

Figure 2.6 Crystal structure of $Na_2Ti_3O_7$ (sodium trititanate).

2.2.3 $K_2Ti_6O_{13}$

The crystal structure of potassium hexatitanate ($K_2Ti_6O_{13}$) is shown in Figure 2.7. It has a monoclinic unit cell with potassium ions inside a tunnel space formed by the TiO_6 octahedral assemblies. The framework is built-up of three TiO_6 octahedra which connect to adjacent layers at the corners [26].

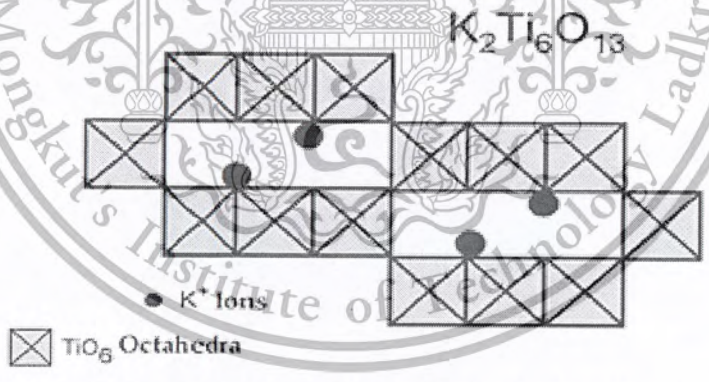

Figure 2.7 Idealized structural of $K_2Ti_6O_{13}$ (potassium hexatitanate).

2.2.4 Li_2TiO_3

Lithium titanate is a compound containing lithium and oxygen. It has the chemical formula Li_2TiO_3. The most common crystallization of Li_2TiO_3 is a monoclinic system. It is also a layered titanate, but of the rock-salt type as shown in Figure 2.8 [27].

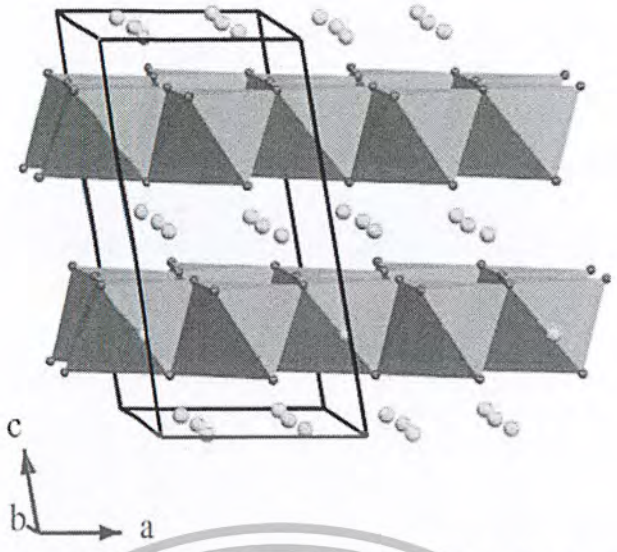

Figure 2.8 Crystal structure of layered rocksalt-type Li_2TiO_3

2.3 Probe molecules to test the basic sites in metal oxides

It is well-known that most metal oxides are strongly basic. They react with water to form basic solutions of the metal hydroxide, or react with an acid to form a salt and water. For example, the basic oxide MgO (magnesium oxide) neutralises sulphuric acid to form magnesium sulphate (salt) and water.

$$MgO_{(s)} + H_2SO_{4\,(aq)} \longrightarrow MgSO_{4\,(aq)} + H_2O_{(l)} \quad \text{Equation 2.1}$$

The base-characters of metal oxides originate from under-coordinated O^{2-} sites on different locations of the crystals. The nanotubes or several layered titanates in the previous section have the basic sites at the interlayer which are accessible to acid molecules. However, the majority of work reports that the basic sites react with typical mineral acids. The behavior of these sites toward other type of acidic probe molecules is unknown.

Some of the acid molecules used in this work are summarized in Figure 2.9 Propanoic acid ($C_3H_6O_2$) has the structure shown in Figure 2.9(a). It is a naturally occurring clear liquid with a pungent and unpleasant smell. The salts and esters of propionic acid are known as propanoates. It is formed when propanoic acid react with basic reactant. Heptanoic acid ($C_7H_{14}O_2$) has structure shown in Figure 2.9(b). It is an oily liquid with an unpleasant smell. It is slightly soluble in water, but very soluble in ethanol and ether. Decanoic acid ($C_{10}H_{20}O_2$) has the structure shown in Figure 2.9(c). It occurs naturally in coconut oil (about 10%) and palm kernel oil (about 4%). Palmitic acid ($C_{16}H_{32}O_2$) has structure shown in Figure 2.9(d). It is the most common fatty acid (saturated) found in palm trees (palm oil), but can also be found in meats, cheeses, butter, and dairy products. Palmitate is a term for the salts and esters of palmitic acid. Fatty acids can be readily obtained from biomass which is abundant in Thailand. Sebacic acid ($C_{10}H_{18}O_4$), has structure shown in Figure 2.9(e). It

is a dicarboxylic acid, having the –COOH group at the two ends of the molecule. Sebacic acid is a derivative of castor oil. In its pure state it is a white flake or powdered crystal.

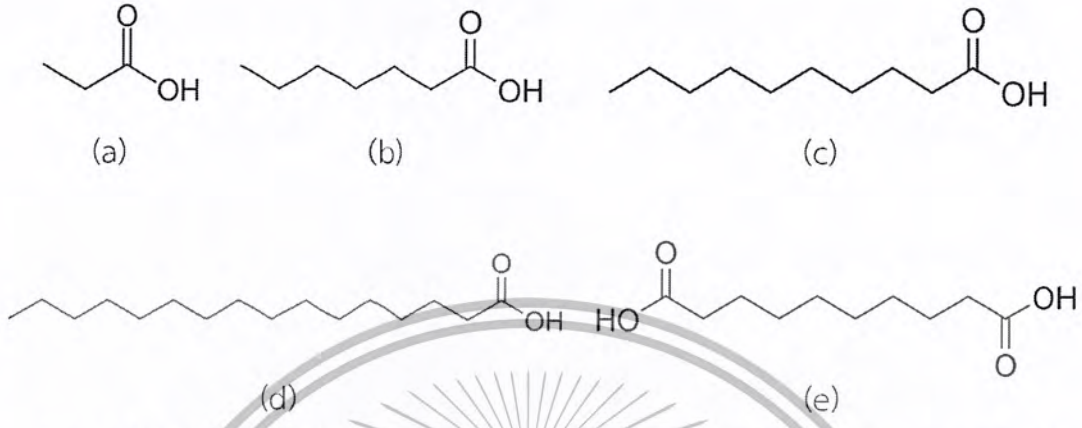

Figure 2.9 Structure of carboxylic acid: (a) propanoic acid, (b) heptanoic acid, (c) decanoic acid, (d) palmitic acid, (e) sebacic acid.

2.4 Literature and Reviews

Yuh et al. [21] has synthesized TNTs by a hydrothermal method at 150 °C for 48 h. After the reaction, precipitates were washed repeatedly using distilled water to be maintained neutral. Some samples were prepared where Na^+ cations were ion-exchanged with H^+ by being dispersed in 0.1 N HCl solution at 60 °C. Scanning electron microscopy (SEM) and transmission electron microscopy (TEM) showed that all of materials have nanotubular shape. BET showed an increase in the specific surface area with the decreases in Na^+ content (by the ion-exchanging process) and in H_2O content (by drying processes). The powders with controlled H_2O and Na^+ contents had high hydrogen uptake of 2.21 wt% at 90 atm.

Ma et al. [6] has soaked protonic titanate nanotubes in 0.1 M alkali metal (Li, Na, K, Rb, Cs) hydroxides at room temperature for 3 days. The soaked sample was centrifuged, washed repeatedly with deionized water and air-dried. The materials were analyzed by XRD. The interlayer spacing of 0.9 nm of the nanotubes after the exchange process remains almost unchanged. So, the interlayer spacing of nanotubes may be more difficult to expand than bulk titanate. This finding is ascribed to the peculiar morphology of TNTs. Also, as shown by TEM, the layered structure of protonic titanate nanotubes can be damaged by electron beam compared to other cations. Ma et al then proposed that intercalated alkali cations play a role in pinning adjacent layers. The elemental maps show the distribution of atomic concentrations of Ti, O and alkali metals in the nanotubes, confirming the ion exchange.

Arsa et al. [23] has adsorbed palmitic acid in isopropanol into the interlayer space of lepidocrocite titanate $K_{0.8}Zn_{0.4}Ti_{1.6}O_4$ by refluxing. Thermogravimetric analysis (TGA) showed that the amount of adsorbed palmitic acid reached 35% by weight. TEM showed that the repeating distance of 0.8 nm in $K_{0.8}Zn_{0.4}Ti_{1.6}O_4$ expanded to 1.2 nm after the adsorption. Fourier transform infrared spectroscopy (FTIR) pointed to the presence of the carboxylate group in the material. It is interesting to see if similar chemistry can occur with TNTs. It is also interesting to see if there is the effect of the chain length of the acid in such chemistry or not.

Wei Wang et al. [28] found that the surface-modified HTNT by caproic acid, capric acid, tetradecanoic acid, hexadecanoic acid and stearic acid maintained the tubular structure. However, the crystal structure of HTNT surface-modified by metacetonic acid transformed into anatase. Through the analysis of FTIR and ARXPS techniques, it was observed that the bonding forms of the surface-modified HTNT were difference. When carbon chains ≤14, the bonding of samples were in both monodentate and bidentate modes; when carbon chain >16, only the monodentate mode was observed. In addition, the PL efficiency of surface-modified HTNT was measured. It was deduced that the bonding forms of carboxylic acid with the surface of HTNT had an effect on the PL efficiency.

CHAPTER 3
EXPERIMENTAL DETAILS

3.1 Reagents

Chemicals	Grade of purity	Manufacturers
1. Titanium dioxide (P25)	-	TOA
2. Sodium hydroxide	≥98%	CARLO ERBA
3. Hydrochloric acid	≥37%	CARLO ERBA
4. Isopropanol	Analysis Grade	CARLO ERBA
5. Propanoic acid	≥98%	CARLO ERBA
6. Heptanoic acid	≥98%	ACROS
7. Decanoic acid	≥99%	ACROS
8. Sebacic acid	≥98%	ACROS
9. Palmitic acid	≥97%	FLUKA

3.2 Apparatus

1. Autoclave
2. Oven
3. Tube furnace
4. Vacuum filter
5. Centrifuge
6. Stirrer and heater
7. Laboratory glassware
8. Laboratory plasticware
9. X-ray powder diffractometer (Rigaku, DMAX 2200/Ultima+, Faculty of Science, Chulalongkorn University)
10. Thermogravimetric analyzer (Perkin-Elmer, Scientific Instrument Service Centre, KMITL)
11. Raman spectrometer (Thermoscientific, DXR Smart Raman, College of Nanotechnology, KMITL)
12. Gas Adsorption Analyzer (Autosorb-1C, Quantachrome, Department of Chemistry, KMITL)
13. Scanning Electron Microscope (SEM JSM-6610 HV/LV with EDX, Faculty of Science, Chulalongkorn University)
14. Attenuated Total Reflection Spectroscopy (Perkin Elmer spectrometer (Spectrum Two) at the resolution of 4 cm^{-1})

3.3 Experimental procedure

3.3.1 Preparation of materials

3.3.1.1 Synthesis of TNTs

The hydrothermal method was employed for the synthesis of TNTs. An amount of 2 g of titanium oxide nanopowder (P25) was dispersed in 100 mL of an aqueous solution of 10 M NaOH [10]. The mixture was then charged into a Teflon-lined autoclave. The autoclave was oven-heated at 160 °C for 48 hours. After that, NaOH was discarded and the product was washed with 0.01 M HCl (3,000 mL), and a sonication with 0.1 M HCl 250 mL for 2 h. The final product were obtained by air-drying at 80 °C and calcination at 300°C for 2 h. In another batch, HCl used for washing was replaced by deionized water.

3.3.1.2 Synthesis of microcrystals of alkali titanates

3.3.1.2.1 $Na_2Ti_3O_7$

$Na_2Ti_3O_7$ (obtained from another group in our laboratory) was prepared by a solid-state reaction with a mixture of Na_2CO_3 and TiO_2 in a molar ratio of 1.1:3 at 800 °C for 40 h, with the intermediate grinding every 20 h [25].

3.3.1.2.2 Lepidocrocite titanate

Lepidocrocite titanate (also obtained from another group in our laboratory) was prepared from a mixture of K_2CO_3, ZnO and TiO_2. The powder was ground and heated at 800°C for 1 hour, followed by a reheating 900°C for 20 hours [29].

3.3.2 Adsorption of carboxylic acid

An amount of 2 g of TNTs was refluxed with 150 mL of a 10%w/w plamitic acid in isopropanol at 60 °C for 36 hours. After completion of the adsorption, the solid was filtered, washed with isopropanol, and dried at 80°C overnight. The material obtained is called "TNTs+palmitic acid". Similar experiment was performed with other acids (10%w/w acid in isopropanol, except sebacic acid which is 5% in isopropanol). A control experiment was also conducted using TNTs and isopropanol, but without the acid. The product from this experiment is called "TNTs+isopropanol"

3.3.3 Determination of adsorption isotherm

The stock solution (75 mL) of 10%w/w heptanoic acid in isopropanol was prepared. The peak area of this stock solution was then determined by a GC, representing the initial concentration of the acid prior to the adsorption.

Then, the adsorption of the acid was performed by refluxing 1 g of the solid with 75 mL of 10%w/w acid in isopropanol. Assuming that the density of the stock solution is 1 g/mL, the initial mass of heptanoic acid is 7.5 g. The liquid was withdrawn at the reaction time t = 0, 1, 2, 3, 4, 5, 6, 12 and 36 h. The liquid was filtered through a syringe filter before the injection into a GC. The peak area of the acid remaining in the mother liquor was then determined. The percentage adsorption at different reaction time was calculated using equation 3.1.

$$\%\text{Adsorption} = \frac{[(\text{Peak area})\ \text{initial} - (\text{Peak area})\ \text{at time t}]}{(\text{Peak area})\ \text{initial}} \times 100\% \quad \text{(Equation 3.1)}$$

Next, %adsorption in equation 3.1 is converted to %mass relative to the initial mass of heptanoic acid in the stock solution. The calculation with decanoic acid can be performed similarly. Details can be found in Appendix B.

3.3.4 Characterization of TNTs and TNTs+carboxylic acid

3.3.4.1 Structural analysis using X-ray diffraction

The crystalline phase of the materials prepared can be identified using Powder X-ray Diffraction (PXRD) measurement. The sample was ground before it was packed on the sample holder. Analysis was done employing Bruker diffractometer (Cu K α radiation, 40 kV, 30 mA), covering the range 2θ = 5-65°, at the rate of 0.02°/step and a scanning rate of 0.6 s/step.

3.3.4.2 Determination of specific surface area by nitrogen adsorption

Surface area of TNTs can be determined by a Gas Adsorption Analyzer (Autosorb-1C, Quantachrome). Approximately, 0.01-0.05 g of the sample was loaded into the cell, which was attached to the outgassing station equipped with a heating mantle. The temperature is raised to 350°C during which the outgassing was conducted. After that, nitrogen gas was introduced to the sample cell where the adsorption can be measured at the range of the partial pressure (P/P_0) from 10^{-6} to 1.0. The adsorption isotherm and the corresponding surface area was analyzed using BET equation as shown in Equation 3.2.

$$\frac{1}{v\left[(p_0/p)-1\right]} = \frac{c-1}{v_m c}\left(\frac{p}{p_0}\right) + \frac{1}{v_m c} \quad \text{(Equation 3.2)}$$

where p and p_0 are the equilibrium and the saturation pressure of adsorbates at the temperature of adsorption, υ is the adsorbed gas quantity (for example, in volume units), υ_m is the monolayer adsorbed gas quantity, and C is the BET constant. This equation has the following hypotheses: (a) gas molecules physically adsorb on a

solid in layers infinitely; (b) there is no interaction between each adsorption layer; and (c) the Langmuir theory can be applied to each layer.

3.3.4.3 Thermal stability of TNTs and TNTs+carboxylic acid

The thermal stability of TNTs was determined from the mass loss after being heated to high temperature, as measured by a Perkin-Elmer thermogravimetric analyzer (Pyris 1). Approximately 10 mg of TNTs was loaded to the platinum plan, after which the exact mass was recorded by the instrument. The sample was then heated from room temperature to 700°C at the heating rate of 10°C/min under the flow of nitrogen gas (20 mL/min). The thermal stability of TNTs+carboxylic acid can be performed similarly.

3.3.4.4 Raman spectroscopy

The powder of the sample to be investigated was manually pressed into the sample holder. Raman spectra were collected using DXR Smart Raman (Thermoscientific) at College of Nanotechnology, KMITL, from 50-4000 cm^{-1}. The laser employed has the wavelength of 532 nm, and the laser power was 5 mW. A total of 15 spectra were collected per one sample, with the exposure time of 2 s each.

3.3.4.5 Scanning electron microscopy

SEM images of TNTs were obtained by a microscope JSM-6610 HV/LV with EDX at Faculty of Science, Chulalongkorn University

3.3.4.6 Attenuated total reflection spectroscopy

ATR spectra of materials were investigated by a FTIR spectra in the attenuated total reflectance (ATR) mode by a Perkin Elmer spectrometer (Spectrum Two) at the resolution of 4 cm^{-1}.

CHAPTER 4
RESULTS AND DISCUSSION

4.1 Materials characterization

4.1.1 SEM

The SEM images of nanotubes sample prepared by a hydrothermal method using P25 as a precursor after the washing with different liquids (HCl and DI water) and calcination at 300 °C for 2 h are shown in Fig. 4.1.

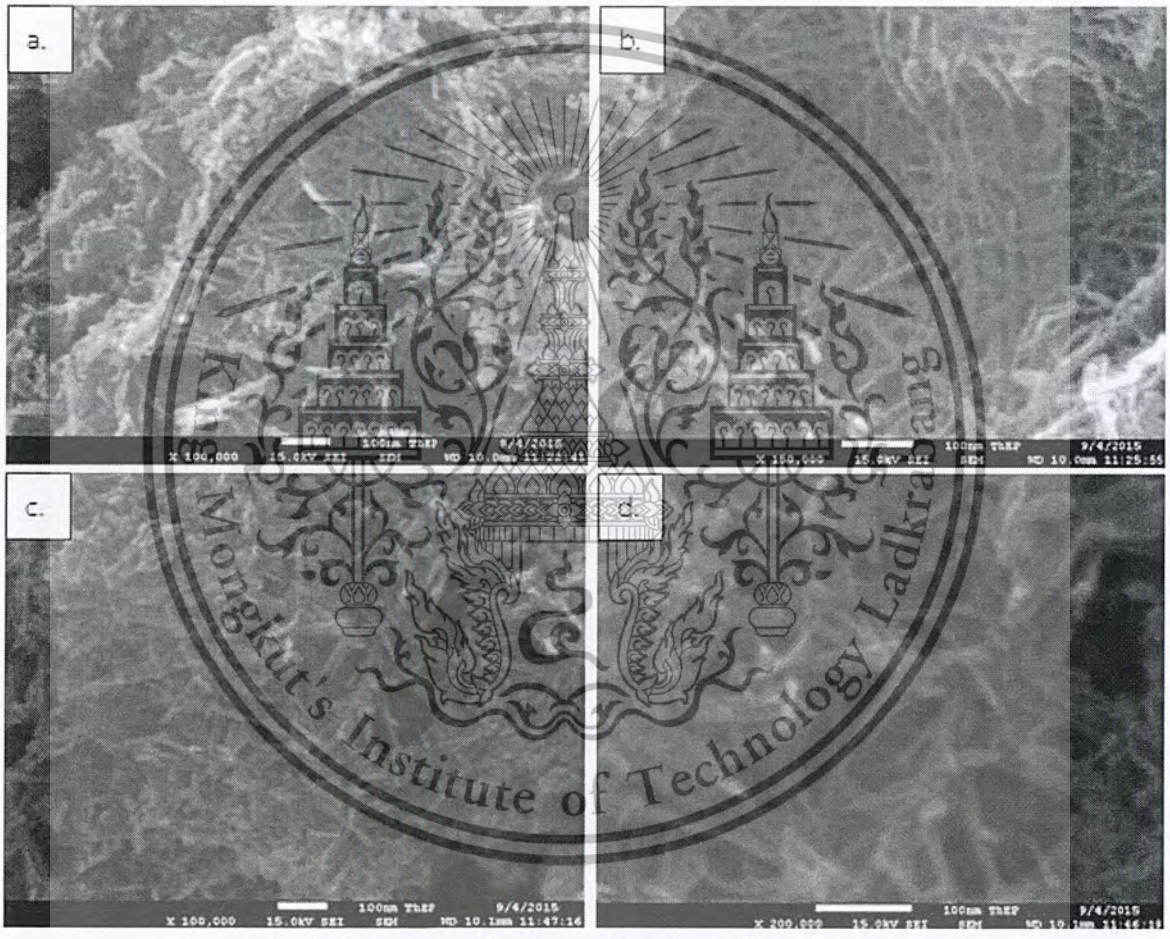

Figure 4.1 SEM images of TNTs-HCl (a,b), or TNTs-DI water (c, d).
All samples were calcined at 300 °C for 2 h.

One can see that the tubular morphology was obtained from both HCl-watched and DI water-washed samples. Interestingly, the length of TNT-HCl washed (Fig. 4.1a,b) is approximately 500 nm, which is longer than that in TNT-DI water washed (Fig. 4.1c,d).

4.1.2 PXRD

The TNTs synthesized were first characterized by powder x-ray diffraction (PXRD) as shown in figure 4.2.

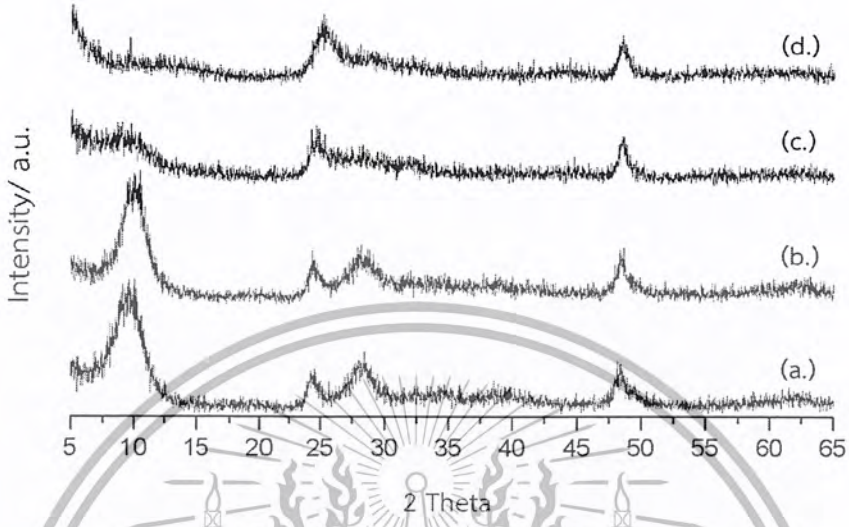

Figure 4.2 PXRD patterns of TNTs-DI water non-calcined (a.), TNTs-DI water calcined (b.), TNTs-HCl non-calcined (c.) and TNTs-HCl calcined (d.).

For the non-calcined TNTs washed with deionized water (Figure 4.2a), peaks at 2theta = 10.0, 24.8 and 48.4 degree can be seen, corresponding to the d spacing at 0.8835, 0.3585 and 0.1878 nm, respectively. The first peak at 2theta = 10.0 degree (d = 0.88 nm) is characteristics of the repeating distance of the titanate sheets which have folded into nanotube. Other peaks detected are also in agreement with the literature [30], indicating the successful synthesis of TNTs via hydrothermal method. Upon calcination (Figure 4.2b), the first peak at 2theta = 10.0 degree (d = 0.8835 nm) was preserved, indicating that TNTs remain intact. Results can be explained considering that the dehydroxylation cannot occur, as Na^+ cations are abundant in the structure. One can infer that the lepidocrocite phase is preserved.

On the contrary, the PXRD of TNTs washed with 1 M HCl upon calcination in Figure 4.2d is different from that shown in Figure 4.2c. The characteristic peak at d = 0.88 nm disappears. This result indicates that the sheets no longer exist. Moreover, the peaks at 2theta = 25.0 and 48.4 (d = 0.3558 and 0.1878nm) are detected, ascribed to the 101 and 200 reflections of anatase [31] respectively. Accordingly, the calcination of TNTs washed with acid transforms the crystal structure from lepidocrocite into anatase, in agreement with the literature [31]. The washing with HCl results in the ion exchange of H^+ (in the acid) with Na^+. Dehydroxylation could therefore occur at high temperature. So, the layered structure collapse and anatase

was formed. The summary of peak positions of all samples can be found in Table 4.1.

Table 4.1 List of 2theta, hkl, and the d spacing of the samples synthesized in this work.

Sample	2theta (degree)	Index (hkl)	d-spacing (nm)
TNTs-DI water non-calcined	10.0	020	0.8835
	24.8	110	0.3585
	28.1	130	0.3172
	48.4	200	0.1878
TNTs-DI water calcined	10.0	020	0.8835
	24.8	110	0.3585
	28.1	130	0.3172
	48.4	200	0.1878
TNTs-HCl non-calcined	10.0	020	0.8835
	24.8	110	0.3585
	48.4	200	0.1878
TNTs-HCl calcined	25.0	101	0.3558
	48.4	200	0.1878

4.1.3 Raman spectroscopy

In order to confirm the PXRD result, The TNTs were then characterized by Raman spectroscopy as shown in figure 4.3.

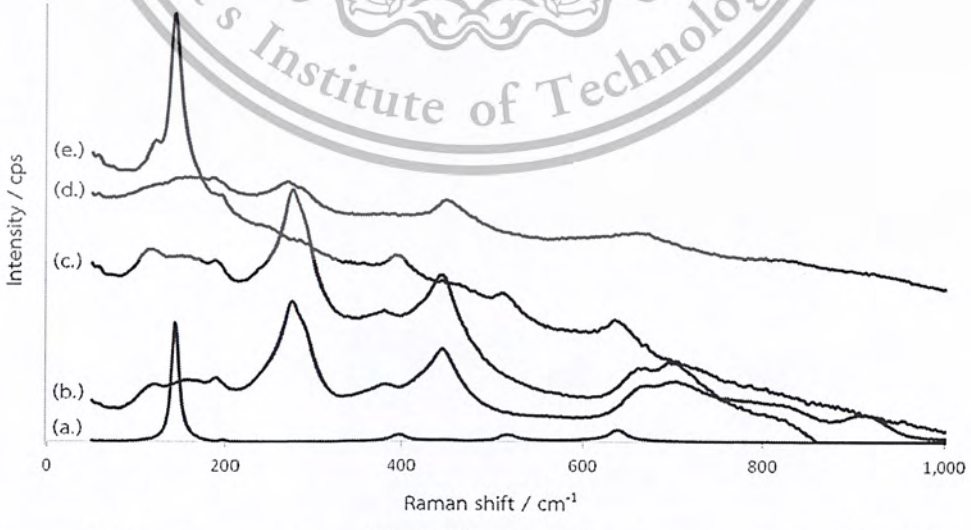

Figure 4.3 Raman spectrum of P25 (a), TNTs-DI water non-calcined (b.), TNTs-DI water calcined (c.), TNTs-HCl non-calcined (d.) and TNTs-HCl calcined (e.).

Fig. 4.3b, c, d show that in TNTs-DI water non-calcined, TNTs-DI water calcined and TNTs-HCl non-calcined, the same peaks at 273, 446 and 662cm^{-1} can be observed. These results are similar to those reported by Kim et al [30]. They ascribed the appearance of Raman peaks at near 440 cm^{-1} to the Ti-O bending, and 660 cm^{-1} to the stretching vibration involving six-coordinated titanium and three-coordinated oxygen. Therefore the crystal structure of lepidocrocite was obtained. After calcination at 300 °C, Fig. 4.3e shows that TNTs-HCl changed and looked like the Raman spectrum of P25, shown in Fig. 4.3a for comparison. However, the spectrum of TNTs-DI water after calcination (Fig. 4.3c) remains relatively unchanged. In short, results from Raman spectroscopy are in good agreement with PXRD measurements.

4.1.4 TGA

The amount of water that was adsorbed in TNTs was determined from thermogravimetric analysis as shown in Fig.4.4.

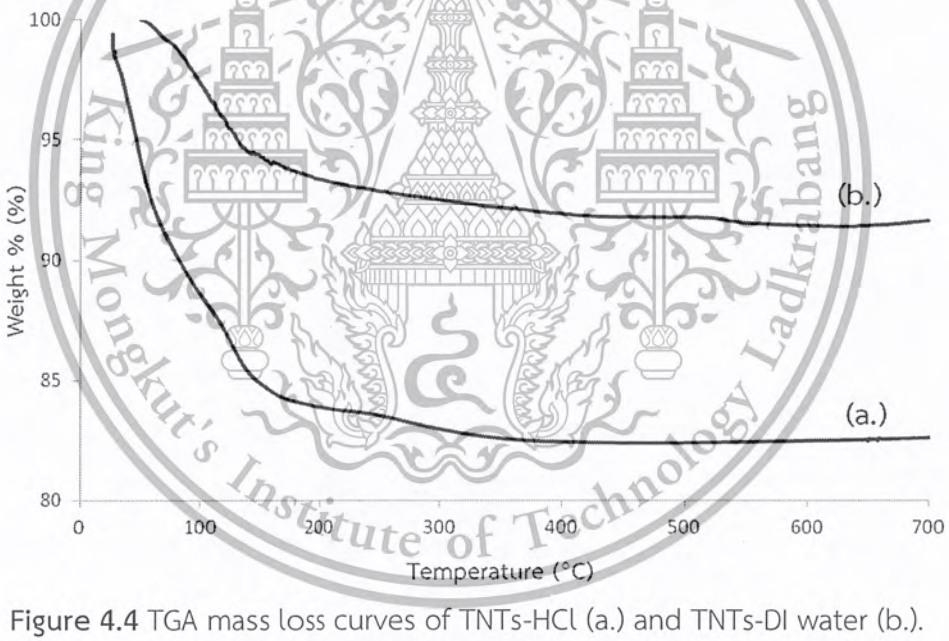

Figure 4.4 TGA mass loss curves of TNTs-HCl (a.) and TNTs-DI water (b.). All samples were calcined at 300 °C for 2 h.

A smaller mass loss at 180-400 °C (7.5%) was observed for TNTs-DI water (Fig. 4.4b.) compared to TNTs-HCl at 50-140 °C (16.8%) (Fig. 4.4a) after calcination at 300 °C for 2 h. The dehydroxylation is unlikely to occur at relatively low temperatures (i.e., starting slightly above RT). So, this mass loss can be ascribed to the adsorption of water molecules from the atmosphere, indicating that TNTs-HCl washed is hygroscopic and the TNTs washed with DI water is less hydroscopic than that washed with HCl.

4.1.5 N_2 adsorption – desorption

The N_2 adsorption-desorption isotherms of TNTs washed with HCl and DI water are shown in Figure 4.5.

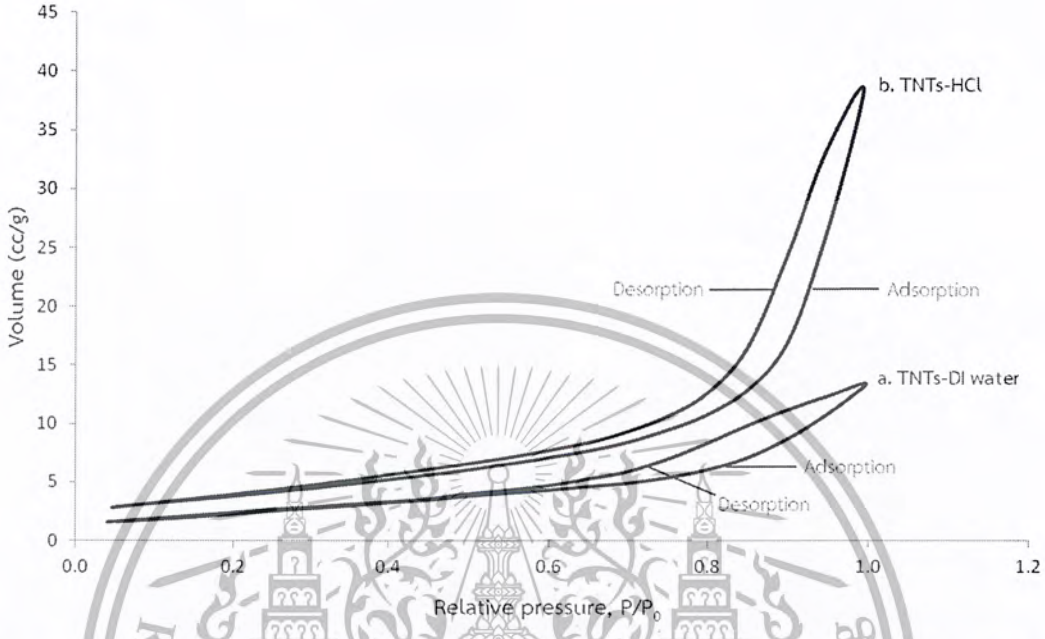

Figure 4.5 N_2 adsorption-desorption isotherm of TNTs-DI water (a) and TNTs-HCl (b). All samples were calcined at 300 °C for 2 h.

These isotherms can be described to type-IV, indicating the presence of mesopores. TNTs washed with HCl has the specific surface area of 363 m^2/g, while the TNTs washed with deionized water has specific surface area of 261 m^2/g. The pore size of TNTs washed with HCl is 18 nm, while that of the TNTs washed with deionized water is 9.5 nm. This indicated that TNTs are mesoporous materials (pore diameter between 2 nm and 50 nm). The pore size distributions of these two samples are shown in Appendix A.

From the N_2 adsorption-desorption isotherm, the shape of the hysteresis loop suggests that TNTs is a mesoporous material. The adsorption and the desorption did not occur at the same pressure. This result can be explained considering the capillary condensation of sorbed N_2 molecules as a result of the confinement between small spaces (a mesopore). That is, the nanotube morphology is preserved regardless of the crystal structure (lepidocrocite or anatase).

4.2 Adsorption

In the recent study [23], organic acid can be adsorbed on the lepidocrocite titanate ($K_{0.8}Zn_{0.4}Ti_{1.6}O_4$) with the expansion of the interlayer by 0.2-0.4 nm. Hence, it

is interesting to investigate the adsorption of organic acid on TNTs-DI water because it retains the lepidocrocite structure after calcination.

Fig. 4.6 shows the adsorption isotherm of TNTs adsorbed with heptanoic acid and decanoic acid.

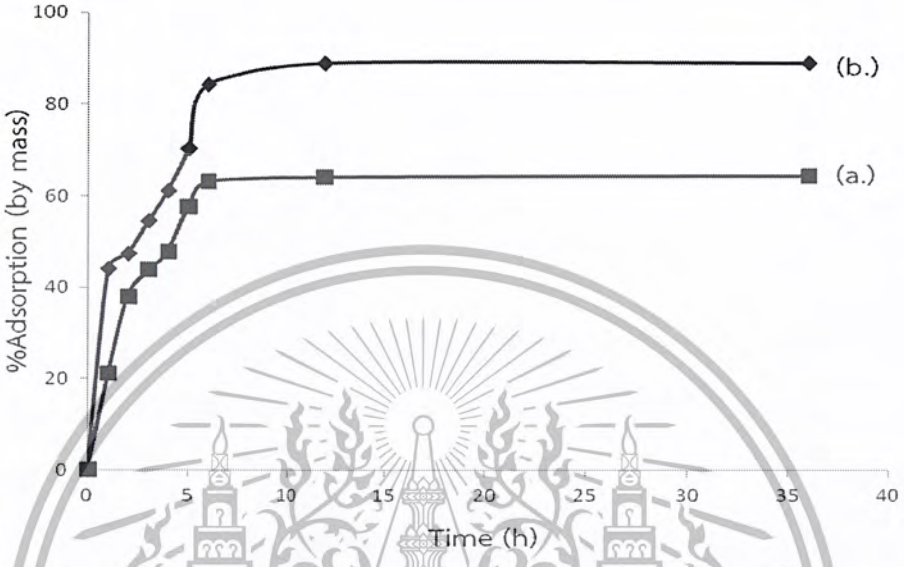

Figure 4.6 The adsorption isotherm of TNTs+heptanoic acid (a) and TNTs+decanoic acid (b).

Adsorption isotherm can be investigated by Gas Chromatography (GC) during the refluxing of TNTs and carboxylic acid using isopropanol as solvent, the solution of carboxylic acid and isopropanol was sampling every hour and detected the loss of carboxylic acid (The calculation shown in Appendix B.)

It can clearly be seen that the adsorption of these acids on TNTs is gradually increased up to 6 h. After that, the adsorption capacity remains constant up to 36 h. The results also indicate that organic acid with longer chain (decanoic acid) can adsorb more readily, as compared to the shorter one (heptanoic acid).

4.3 Effect of titanate adsorbent

4.3.1 TGA

TNTs, $K_{0.8}Zn_{0.4}Ti_{1.6}O_4$ (Lepidocrocite titanate) and related structures were tested for the adsorption of organic acid by refluxing at 60 °C for 36 h. The samples were then washed with isopropanol and dried at 80 °C. The amount of adsorbed acid was investigated by TGA, as shown in Table 4.2

Table 4.2 Surface area, Sanderson intermediate electronegativity, partial negative charges of framework oxygen, % mass loss and decomposition temperature of materials after adsorption of heptanoic acid.

Sample	Surface area (m^2/g)	Sanderson intermediate electro-negativity (S_{int})	Partial negative charges of framework oxygen (σ_1)	% Mass loss and Temperature part 1	% Mass loss and Temperature part 2	% Mass loss and Temperature part 3	Total mass loss
TNTs	261	N/A	N/A	9.8% 64-133 °C	1.9% 306 °C	1.2% 408 °C	12.9%
KZn	3	2.7529	-0.5175	-	1.4% 261 °C	-	1.4%
Li_2TiO_3	10	2.1837	-0.6374	-	8.6% 262 °C	3.6% 317 °C	12.2%
$Na_2Ti_3O_7$	66	2.6845	-0.5319	-	0.9% 211 °C	3.1% 345 °C	4.0%
$K_2Ti_6O_{13}$	12	2.8160	-0.5042	-	1.4% 301 °C	-	1.4%

From Table 4.2, there are three parts of weight loss. As the samples were washed with isopropanol, the first is the desorption of solvent. The second part is the mass loss of carboxylic acid that adsorbs on the external surface. The last one is the mass loss of carboxylic acid adsorbed on the internal surface where the decomposition temperature is higher than the boiling point of free carboxylic acid.

Considering heptanoic acid adsorped on the internal surfaces, the adsorption of the acid on Li_2TiO_3 is higher than that on other materials. This is because Li_2TiO_3 closes high basicity (The basicity of materials was calculated by Sanderson intermediate electronegativity and partial negative charges of framework oxygen as shown in APPENDIX E) [32]. Accordingly, Li_2TiO_3 surface would strongly interact with the carboxylic acid. It can be seen that the adsorption of carboxylic acid depending on basicity as shown in Fig. 4.7. This study suggests that surface area of material does not affect the adsorption capacity of carboxylic acid.

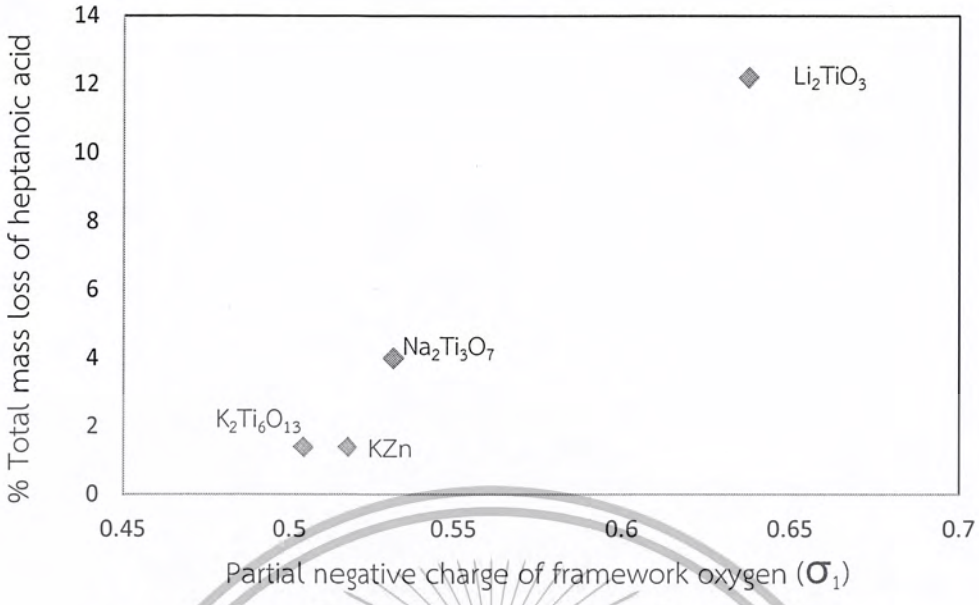

Figure 4.7 The relation of % total mass loss of heptanoic acid and Partial negative charge of framework oxygen (σ_1)

4.3.2 ATR

Figure 4.8 shows the ATR spectra of TNTs and some other alkali titanates refluxed with heptanoic acid at 60 °C for 36 h. After refluxed, the powder was washed with isopropanol and dried at 80 °C.

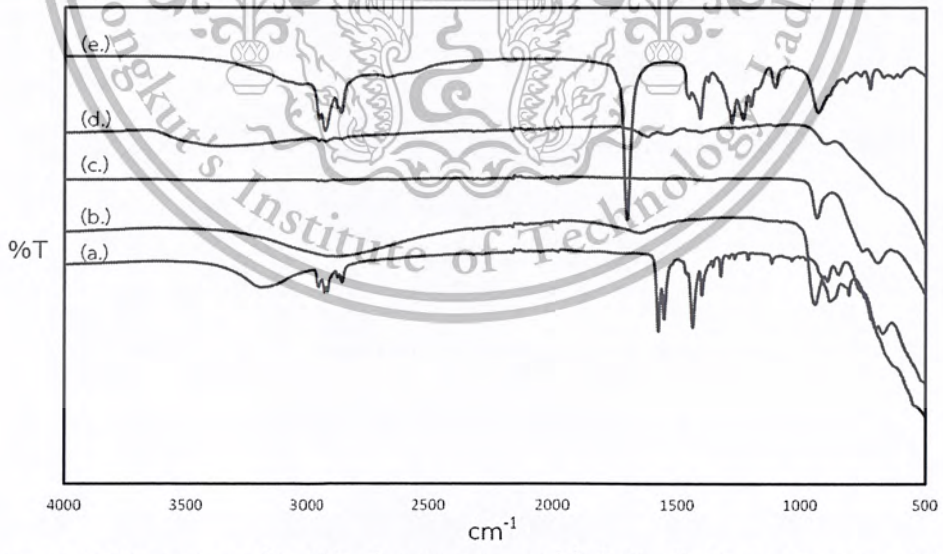

Figure 4.8 ATR spectra of Li_2TiO_3+heptanoic acid (a.), $Na_2Ti_3O_7$+heptanoic acid (b.), $K_2Ti_6O_{13}$+heptanoic acid (c.), TNTs+heptanoic acid (d.), Heptanoic acid (e.)

The characteristic peak of heptanoic acid (Fig. 4.8e) includes the peak at around 2800 cm^{-1} assigned to the C-H stretching of alkyl of heptanoic acid and the peak around 1700 cm^{-1} which refer to the stretching of C=O. ATR spectra of

Li_2TiO_3+heptanoic acid (Fig. 4.8a) and TNTs+heptanoic acid (Fig. 4.8d) show the peak at 2800 cm^{-1} and the corresponding peak at 1600 cm^{-1}. These peaks are assigned to the heptanoate salt. For carboxylate anions, the vibration of C=O will shift to the lower wavenumber as compared to the respecttive vibration of C=O in parent carboxylic acid [23]. From this result, it confirms that heptanoic acid adsorbed on TNTs and Li_2TiO_3.

4.4 Effect of carboxylic acid in TNTs

4.4.1 TGA of TNTs+carboxylic acid

After the adsorption of TNTs and organic acid by refluxing at 60 °C for 36 h, the powder was washed with isopropanol and dried at 80 °C. The amount of adsorbed acid was investigated by thermogravimetric analysis (TGA) as shown in Table 4.3.

Table 4.3 % Mass loss and decomposition temperature of product after adsorption of carboxylic acids on TNTs.

Sample	% Mass loss and Temperature part 1	% Mass loss and Temperature part 2	% Mass loss and Temperature part 3	Total mass loss
TNTs+isopropanol (Blank)	9.6% 131 °C	-	-	9.6%
TNTs+propanoic acid	11.1% 54-141 °C	1.7% 315 °C	-	12.8%
TNTs+heptanoic acid	9.8% 64-133 °C	1.9% 306 °C	1.2% 408 °C	12.9%
TNTs+decanoic acid	9.2% 125 °C	2.3% 274 °C	1.9% 378 °C	13.4%
TNTs+palmitic acid	10.7% 55-132 °C	2.3% 284 °C	3.8% 438 °C	16.8%
TNTs+sebacic acid	3.8% 135 °C	3.6% 280 °C	10.0% 441 °C	17.4%

From Table 4.3, the first mass loss is the desorption of isopropanol at external and internal surface (54-141 °C). The second mass loss is the adsorption of carboxylic acid on the external surface (274-315 °C). The third mass loss (378-441 °C)

is the adsorption of carboxylic acid on the internal surface where the decomposition temperature is higher than boiling point of free carboxylic acid.

Considering the adsorption on internal surface of TNTs, apparently the adsorption of long chain carboxylic acids is higher than that of short chain carboxylic acids.

The TGA of TNTs adsorbed with sebacic acid shows the mass loss higher than decanoic acid (Sebacic acid has the same number of carbon atoms with decanoic acid, but has two carboxylic groups instead of one). This can be ascribed to the presence of dicarboxylic acids having the interactions with the TNTs, as compared to the monocarboxylic acid.

4.4.2 ATR of TNTs+carboxylic acid

The adsorption of carboxylic acid on TNTs washed with DI water can be investigated using Attenuated total reflection (ATR) spectroscopy as shown in Fig. 4.9.

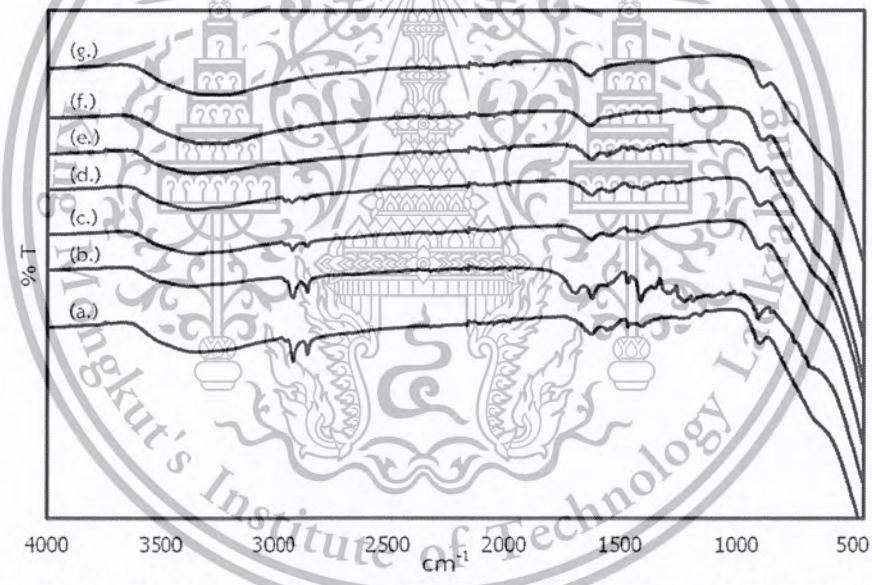

Figure 4.9 ATR spectra of TNTs+palmitic acid (a.), TNTs+sebacic acid (b.), TNTs+decanoic acid (c.), TNTs+heptanoic acid (d.), TNTs+propanoic acid (e.), TNTs+isopropanol (Blank) (f.) and TNTs-DI water (g.).

Figure 4.9g shows the spectrum of TNTs-DI water washed. The peak at 920 cm^{-1} can be attributed to the Ti-O stretching mode [33]. The peak at 1690 cm^{-1} can be assigned to the H-O-H deformation mode of water molecules and the peak at 3425 cm^{-1} can be refer to the stretching vibrations of hydroxyl group of adsorbed water. The presence of the hydroxyl groups (water molecules) is in agreement with TGA results.

The spectrum of the nanotubes after being refluxed with isopropanol (i.e., "Blank", Figure 4.9f) was similar to TNTs. There are no detectable changes due to the treatment with isopropanol. The products obtained after the adsorption with different organic acids (Fig. 4.9a-e) show the ATR spectra sharing some common features. The peaks at 3425, 1690 and 920 cm^{-1} are maintained, while some new bands evolved. The adsorption of propanoic acid on TNTs shows the weak peaks at 2940 and 2900 cm^{-1}, which are characteristics of the C-H stretching. These two peaks get stronger as the molecular weight of the acid is increased (from propanoic acid to palmitic acid).

4.4.3 PXRD of TNTs+carboxylic acid

The PXRD patterns of TNTs after the adsorption with carboxylic acids are shown in Figure 4.10.

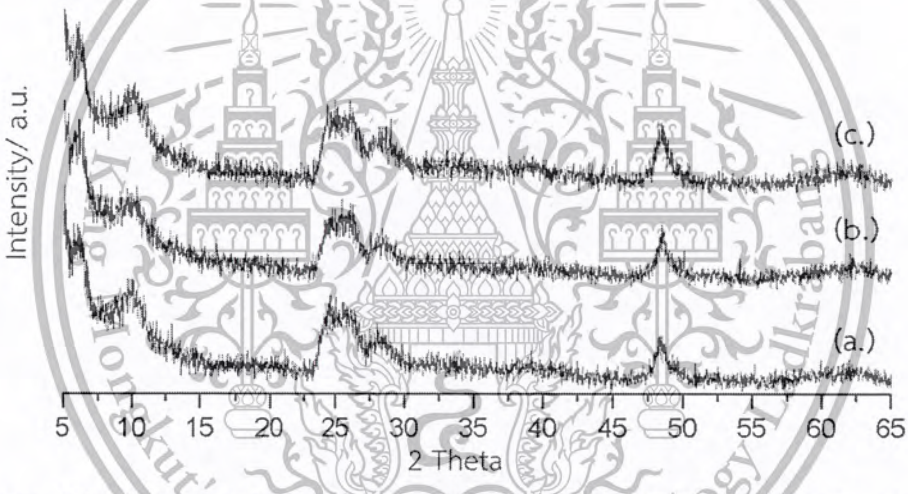

Figure 4.10 PXRD patterns of TNTs+palmitic acid (a.), TNTs+heptanoic acid (b.), and TNTs+propanoic acid (c.).

The summary of 2theta, hkl, and the d spacing of TNTs after the adsorption with carboxylic acid is shown in Table 4.4. The peak positions are generally similar, with peaks at 2θ = 10°, 24.8°, 28.1° and 48.4°, indexed as the 020, 110, 130 and 200 reflections, respectively. The first peak at 2θ = 10° (d = 0.88 nm) is characteristics of the protonic titanates [28], where H^+ replaces Na^+. This finding indicates that the expansion of TNTs layer does not occur after adsorption of carboxylic acids with different carbon chain length.

Table 4.4 List of 2theta, hkl, and the d spacing of the samples in this work.

Sample	2theta (degree)	Index (hkl)	d-spacing (nm)
TNTs+10%w/w propanoic acid	10.0	020	0.8835
	24.8	110	0.3585
	28.1	130	0.3172
	48.4	200	0.1878
TNTs+10%w/w heptanoic acid	10.0	020	0.8835
	24.8	110	0.3585
	28.1	130	0.3172
	48.4	200	0.1878
TNTs+10%w/w palmitic acid	10.0	020	0.8835
	24.8	110	0.3585
	28.1	130	0.3172
	48.4	200	0.1878

4.5 Effect of carboxylic acid in lepidocrocite titanate

4.5.1 TGA of lepidocrocite titanate+carboxylic acid

After adsorption of carboxylic acid by refluxing at 60 °C for 36 h, the powder was washed with isopropanol and dried at 80 °C. The sample was characterized by thermogravimetric analysis (TGA), as shown in Table 4.5.

Table 4.5 % Mass loss and decomposition temperature of product after adsorption of carboxylic acids on lepidocrocite titanate $K_{0.8}Zn_{0.4}Ti_{1.6}O_4$ "KZn".

Sample	% Mass loss and Temperature part 1	% Mass loss and Temperature part 2	% Mass loss and Temperature part 3	Total mass loss
KZn+propanoic acid	-	1.0% 255 °C	-	1.0%
KZn+heptanoic acid	-	1.4% 261 °C	-	1.4%
KZn+sebacic acid	-	13.2% 261 °C	2.7% 422 °C	15.9%

From Table 4.5, The first part shows weakly physisorbed isopropanol on KZn. The next one is the mass loss of carboxylic acid adsorbed on the external surface (255-261 °C). The last one is the mass loss of carboxylic acid adsorbed on the

internal surface (422 °C) where the decomposition temperature is higher than boiling point of free carboxylic acid.

For KZn adsorbed with propanoic acid and heptanoic acid, only small mass losses at 255 °C and 261 °C were observed. This suggests that propanoic acid and heptanoic acid dose not adsorb on KZn. For sebacic acid, three parts of the mass loss are observed. Clearly the presence of two carboxylic groups could promote the adsorption. The total mass loss, i.e., the uptake of sebacid acid, is 34.4% mostly on external surface (23.3%) and some on internal surface (9.4%). Although the specific surface area of KZn (3 m^2/g) is very small, as compared to that of TNTs washed with water (261 m^2/g), the uptake of sebacic acid in KZn is comparable to that in TNTs (17.4%) mostly on external surface (3.6%) and some on internal surface (10.0%).

4.5.2 PXRD of lepidocrocite titanate+carboxylic acid

The PXRD patterns of KZn, including the product after the adsorption of some acids, are shown in Fig. 4.11.

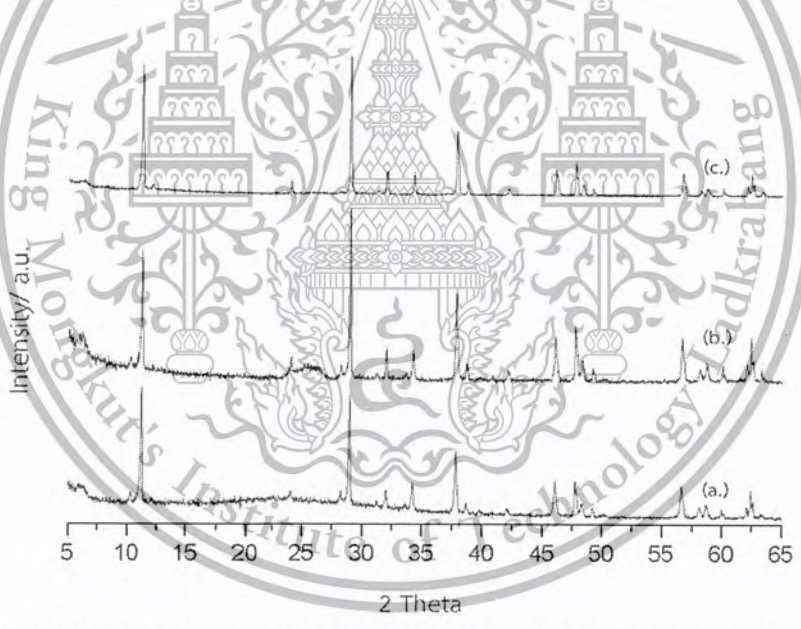

Figure 4.11 PXRD patterns of lepidocrocite titanate+heptanoic acid (a.), lepidocrocite titanate+propanoic acid (b.) and lepidocrocite titanate KZn (c.).

In all cases, the most prominent peak is at 2theta of 11.3 degree (d-spacing 0.7821 nm). The whole pattern is characteristics of the lepidocrocite titanate [23]. The similarity in the PXRD patterns is in agreement with TGA results, where very small amount of the acids were taken by the internal surface of the material. Therefore, the interlayer separation cannot be observed.

It has been recently reported [23] that the adsorption of palmitic acid results in the swelling of KZn by 0.1 nm. Interestingly, such limited expansion is not

observed in this work with heptanoic acid and propanoic acid. This result suggests that a hydrophobic-hydrophobic interaction between the hydrocarbon chains plays a significant role in swelling.

CHAPTER 5
CONCLUSION AND SUGGESTION

5.1 Conclusion

The titanate nanotubes (TNTs) were prepared by a hydrothermal method. The crystal structure of as-made TNTs is lepidocrocite, regardless of the liquid used during washing (deionized water or HCl). After calcination at 300 °C for 2 h, however, TNTs washed with HCl have changed from lepidocrocite into anatase phase due to the dehydroxylation at high temperature. On the other hand, the lepidocrocite structure is preserved after calcination for the TNTs washed with deionized water, likely because the presence of Na^+ cations limits the dehydroxylation. The change in the crystal structure detected by PXRD is also confirmed by Raman measurement.

The adsorption of a carboxylic acid onto several alkali titanates with related structure has also been investigated taking heptanoic acid as a representative. The materials tested include lepidocrocite titanate microcrystals $K_{0.8}Zn_{0.4}Ti_{1.6}O_4$, step-three layered titanate $Na_2Ti_3O_7$, layered Li_2TiO_3, and $K_2Ti_6O_{13}$ with the tunnel structure. The titanates were refluxed with heptanoic acid at 60 °C for 36 hours and washed with isopropanol. The extent of adsorption of heptanoic acid varies, likely reflecting the basicity of the titanate and also the steric hindrance. Among different structures, the highest amount of adsorbed heptanoic acid (external surface, 8.6%; internal surface, 3.6%) is on Li_2TiO_3. The high basicity of Li_2TiO_3 is suggested by the partial negative charges of framework oxygen as calculated by Sanderson intermediate electronegativity.

The TNTs washed with deionized water were further tested for their adsorption behavior toward several carboxylic acids, in order to study the interactions between the O^{2-} basic sites in TNTs and the acid sites in the carboxylic acid. The adsorption of carboxylic acids on TNTs was investigated combining TGA, GC, ATR, and PXRD analysis. The TNTs were refluxed with the acids at 60 °C for 36 hours and washed with isopropanol. We found that there are two adsorption sites on TNTs, i.e., external and internal surfaces. The influence of the molecular structure of the acids affecting the adsorption has been demonstrated as well. For acids that have the same number of carbon atoms, it was found that TNTs can adsorb a larger amount (17.4%) of di-carboxylic acid (sebacic acid, $(HCOO)C_8H_{16}(COOH)$) compared to 7.3% of the mono-carboxylic acid (decanoic acid, $C_9H_{19}COOH$). This result can be explained considering that the di-carboxylic acid has two acid sites (per molecule) which can interact with O^{2-} sites of TNTs. Moreover, we found that TNTs can adsorb a higher concentration of long chain carboxylic acid, as compared to the shorter one.

For example, the adsorption of palmitic acid (C16 acid) is as large as 16.8%, while the adsorption of propionic acid (C3 acid) is as small as 12.8%. From PXRD analysis, one can conclude that after the adsorption of carboxylic acids, the layers of TNTs do not expand. Also, using several carboxylic acids with different number of carbon atoms do not affect the distance between the layers, likely because of the strain inherent to TNTs.

5.2 Suggestion

5.2.1 These materials showing adsorption toward carboxylic acids might be catalytically active for the conversion of carboxylic acids to products of high commercial value. The catalytic activity of these materials could be investigated further.

5.2.2 The adsorption of other organic acids such as alkyl phosphonic acids and alkyl sulfonic acids should be investigated in more details, including the variation of the molecular structure of the acids, the temperature and time profile of the adsorption, to gain more insight into the adsorption behavior.

REFERENCES

[1] Chung Leng Wong, Yong Nian Tan, Abdul Rahman Mohamed. 2011. "A review on the formation of titania nanotube photocatalysts by hydrothermal treatment." *Journal of Environmental Management.* 92 : 1669-1680.

[2] Y. Okour, H.K. Shon, I.J. El Saliby, R. Naidu, J.B. Kim, J.-H. Kim. 2010. "Preparation and characterisation of titanium dioxide (TiO_2) and thiourea-doped titanate nanotubes prepared from wastewater flocculated sludge." *Bioresource Technology.* 101 : 1453-1458.

[3] Huogen Yu, Jiaguo Yu, Bei Cheng, Jun Lin. 2007. "Synthesis, characterization and photocatalytic activity of mesoporous titania nanorod/titanate nanotube composites." *Journal of Hazardous Materials.* 147 : 581–587.

[4] Yean Ling Pang, Steven Lim, Hwai Chyuan Ong, Wen Tong Chong. 2014. "A critical review on the recent progress of synthesizing techniques and fabrication of TiO_2-based nanotubes photocatalysts" *Applied Catalysis A: General.* 481 : 127–142.

[5] Nan Liu, Xiaoyin Chen, Jinli Zhang, Johannes W. Schwank. 2014. "A review on TiO_2-based nanotubes synthesized via hydrothermal method: formation mechanism, structure modification, and photocatalytic applications." *Catalysis Today.* 225 : 34– 51.

[6] Renzhi Ma, Takayoshi Sasaki, Yoshio Bando. 2005. "Alkali metal cation intercalation properties of titanate nanotubes" *Chemical Communications.* 7 : 948–950.

[7] Xiaoming Sun, Yadong Li. 2003. "Synthesis and characterization of ion-exchangeable titanate nanotubes." *Chemistry - A European Journal.* 9 : 2229 – 2238.

[8] H.Y. Zhu, Y. Lan, X.P. Gao, S.P. Ringer, Z.F. Zheng, D.Y. Song, J.C. Zhao. 2005. "Phase transition between nanostructures of titanate and titanium dioxides via simple wet-chemical reactions." *Journal of the American Chemical Society.* 127 : 6730–6736.

[9] Y.Q. Wang, G.Q. Hu, X.F. Duan, H.L. Sun, Q.K. Xue. 2002. "Microstructure and formation mechanism of titanium dioxide nanotubes." *Chemical Physics Letters.* 365 : 427–431.

[10] LI Zhenhua, LIU Zhongqing, YAN Qingzhi, WANG Yichao, and GE Changchun. 2008. "Preparation and performance of titanate nanotube by hydrothermal treatment." *Rare Metals.* 27 : 187-191.

[11] Ashraf. M. El Saeed, M. Abd El- Fattah, M.M. Dardir. 2015. "Synthesis and characterization of titanium oxide nanotubes and its performance in epoxy nanocomposite coating." *Progress in Organic Coatings.* 78 : 83–89.

[12] Q. Chen, G.H. Du, S. Zhang, L.-M. Peng. 2002. "The structure of trititanate nanotubes" *Acta Crystallographica Section B Structural Science.* 58 : 587–593.

[13] B. Liu, E.S. Aydil. 2009. "Growth of oriented single-crystalline rutile TiO_2 nanorods on transparent conducting substrates for dye-sensitized colar cells." *Journal of the American Chemical Society.* 131 : 3985–3990.

[14] L.-Q. Weng, S.-H. Song, S. Hodgson, A. Baker, J. Yu. 2006. "Synthesis and characterisation of nanotubular titanates and titania." *Journal of the European Ceramic Society.* 26 : 1405–1409.

[15] Q. Chen, W. Zhou, G.H. Du, L.-M. Peng. 2002. "Trititanate nanotubes made via a single alkali treatment." *Advanced Materials.* 14 : 1208–1211.

[16] M. Zhang, Z. Jin, J. Zhang, X. Guo, J. Yang, W. Li, X. Wang, Z. Zhang. 2004. "Effect of annealing temperature on morphology, structure and photocatalytic behavior of nanotubed $H_2Ti_2O_4(OH)_2$." *Journal of Molecular Catalysis A: Chemical.* 217 : 203–210.

[17] D.V. Bavykin, J.M. Friedrich, F.C. Walsh. 2006. "Protonated titanates and TiO_2 nanostructured materials: synthesis, properties, and applications." *Advanced Materials.* 18 : 2807–2824.

[18] H.-K. Seo, G.-S. Kim, S.G. Ansari, Y.-S. Kim, H.-S. Shin, K.-H. Shim, E.-K. Suh. 2008. "A study on the structure/phase transformation of titanate nanotubes synthesized at various hydrothermal temperatures." *Solar Energy Materials & Solar Cells.* 92 : 1533–1539.

[19] Wang, B.X., Xue, D.F., Shi, Y., Xue, F.H. 2008. "Titania 1D nanostructured materials: synthesis, properties and applications." In: Prescott, W.V., Schwartz, A.I. (Eds.), Nanorods, Nanotubes and Nanomaterials Research Progress. New Nova Science Publishers Inc., New York, pp. 163-201.

[20] D.V. Bavykin, M. Carravetta, A.N. Kulak, F.C. Walsh. 2010. "Application of magic-angle spinning NMR to examine the nature of protons in titanate nanotubes." *Chemistry of Materials.* 22 : 2458–2465.

[21] Junhan Yuh, and Wolfgang M. Sigmund. 2015. "Room temperature hydrogen uptake of titanate nanotube powder with different H_2O and sodium contents synthesized by a hydrothermal methodin aqueous NaOH solution. *Journal of Ceramic Processing Research.* 16 : 74-80.

[22] S. Papp, I. Dékány. 2005. "Colloid chemical characterisation of layered titanates, their hydrophobic derivatives and self-assembled films." *Colloid and Polymer Science*. 283 : 1116–1122.

[23] Maluangnont, T. Arsa, P. Limsakul, K. Juntarachairot, S. Sangsan, S. Kazuma, G. Sooknoi, T. 2016. "Surface and interlayer base-characters in lepidocrocite titanate: The adsorption and intercalation of fatty acid." *Journal of Solid State Chemistry*. 238 : 175-181

[24] Yongsheng Wei, Liangbo Shen, Zhongming Wang, Wein-Duo Yang, Hong Zhu 2011. "A novel membrane for DMFC - $Na_2Ti_3O_7$ nanotubes/Nafion® composite membrane." *International Journal of Hydrogen Energy*. 36 : 5088–5095.

[25] Bizhou Lin, Yi Zhou, Liwen He, Weiwei Yang, Yilin Chen, Bifen Gao. 2015. "Mesoporous CdS-pillared $H_2Ti_3O_7$ nanohybrids with efficient photo-catalytic activity." *Journal of Physics and Chemistry of Solids*. 79 : 66-71.

[26] Hilda Cm-Dresdner, M. J. Buerger. 1962. "The crystal structure of potassium hexatitanate $K_2Ti_6O_{13}$." *Zeitschrift fiir Kristallographie*. 117 : 411-430.

[27] Andreas Laumann, Karl Thomas Fehr, Martin Wachsmann, Michael Holzapfel, Bo Brummerstedt Iversen. 2010. "Metastable formation of low temperature cubic Li_2TiO_3 under hydrothermal conditions — Its stability and structural properties." *Solid State Ionics*. 181 : 1525–1529.

[28] Wei Wang, Jingwei Zhang, Huizhong Huang, Zhishen Wu, Zhijun Zhang. 2008. "Surface-modification and characterization of H-titanate nanotube." *Colloids and Surfaces A: Physicochem. Eng. Aspects*. 317 : 270–276.

[29] Kaewmora, P. Maneerattanaamorn, W. Netrungruang, W. 2014. "Preparation of self-cleaning glass by coating with lepidocrocite titanate nanosheets." A Special project for The Degree of Bachelor of Science, Industrial Chemistry Program, Faculty of Science, King Mongkut's Institute of Technology Ladkrabang.

[30] Renzhi Ma, Katsutoshi Fukuda,Takayoshi Sasaki, Minoru Osada, Yoshio Bando. 2005. "Structural features of titanate nanotubes/nanobelts revealed by raman, x-ray absorption fine structure and electron diffraction characterizations." *The Journal of Physical Chemistry*. 109 : 6210-6214.

[31] Huiyu Yuan, Rogier Besselink, Zhaoliang Liao, Johan E. ten Elshof. 2014. "The swelling transition of lepidocrocite-type protonated layered titanates into anatase under hydrothermal treatment." *Scientific Reports*. 4(4584) : 1-6.

[32] R.T.Sanderson. "Chemical bond and bond energy." Department of chemistry, Arizona state university. 1976. pp. 41.

[33] Carolina M. Rodrigues, Odair P. Ferreira and Oswaldo L. Alves. 2010. "Interaction of sodium titanate nanotubes with organic acids and base: chemical, structural and morphological stabilities" *Journal of the Brazilian Chemical Society.* 21 : 1341-1348.

APPENDICES

APPENDIX A

MATERIALS CHARACTERIZATION

Quantachrome Corporation
Quantachrome Autosorb Automated Gas Sorption System Report
Autosorb for Windows® Version 1.19

Sample ID	H2 storage T batch1				
Description	Ads 22 Pts Des 22 Pts BET 11 pts				
Comments					
Sample Weight	0.0386 g				
Adsorbate	NITROGEN	Outgas Temp	300.0 °C	Operator	Nook
Cross-Sec Area	16.2 Å²/molecule	Outgas Time	23.9 hrs	Analysis Time	753.2 min
NonIdeality	6.580E-05	P/Po Toler	2	End of Run	08/26/2015 10:1
Molecular Wt	28.0134 g/mol	Equil Time	3	File Name	580825_2.RAW
Station #	1	Bath Temp.	77.35		

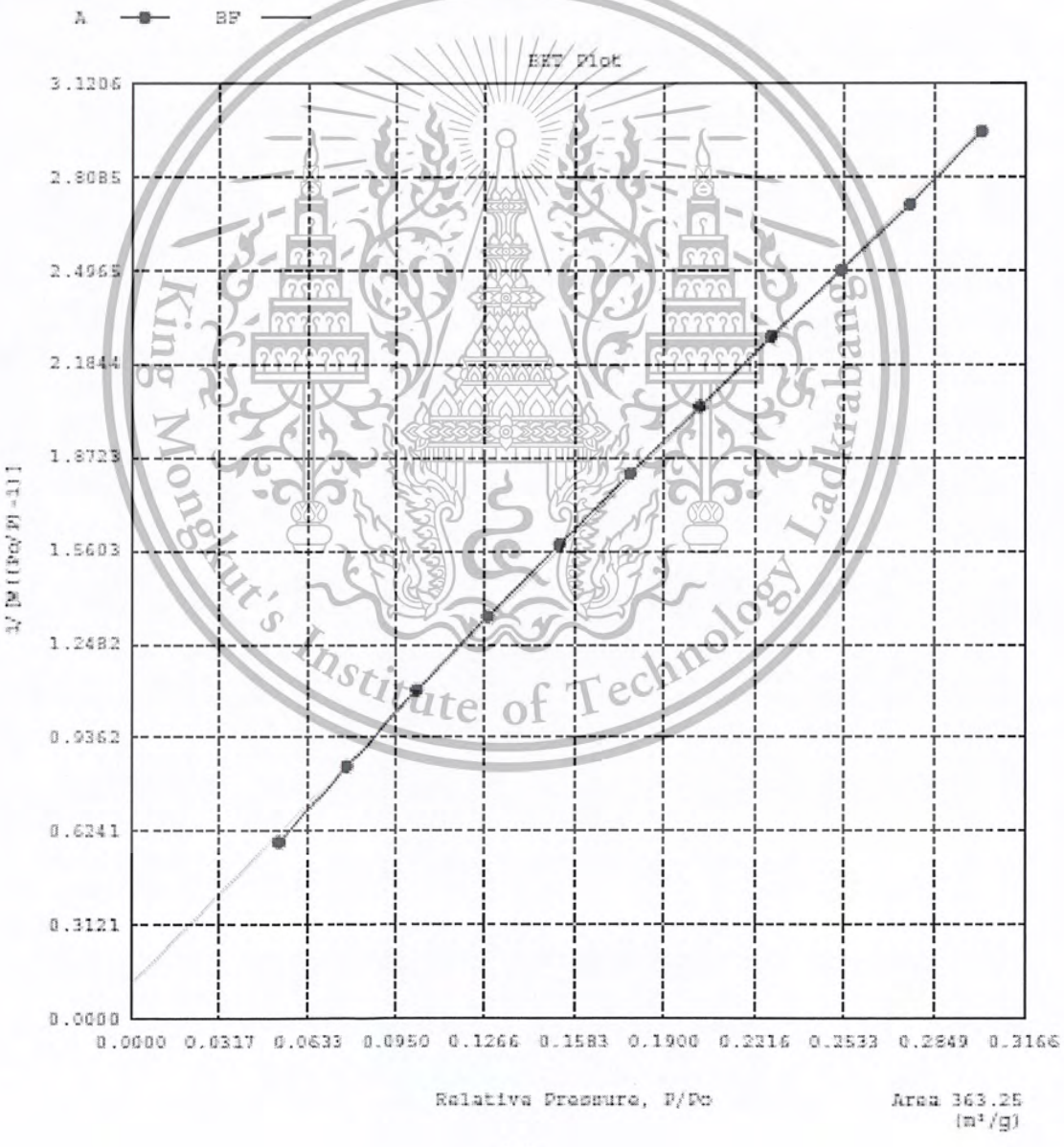

(a)

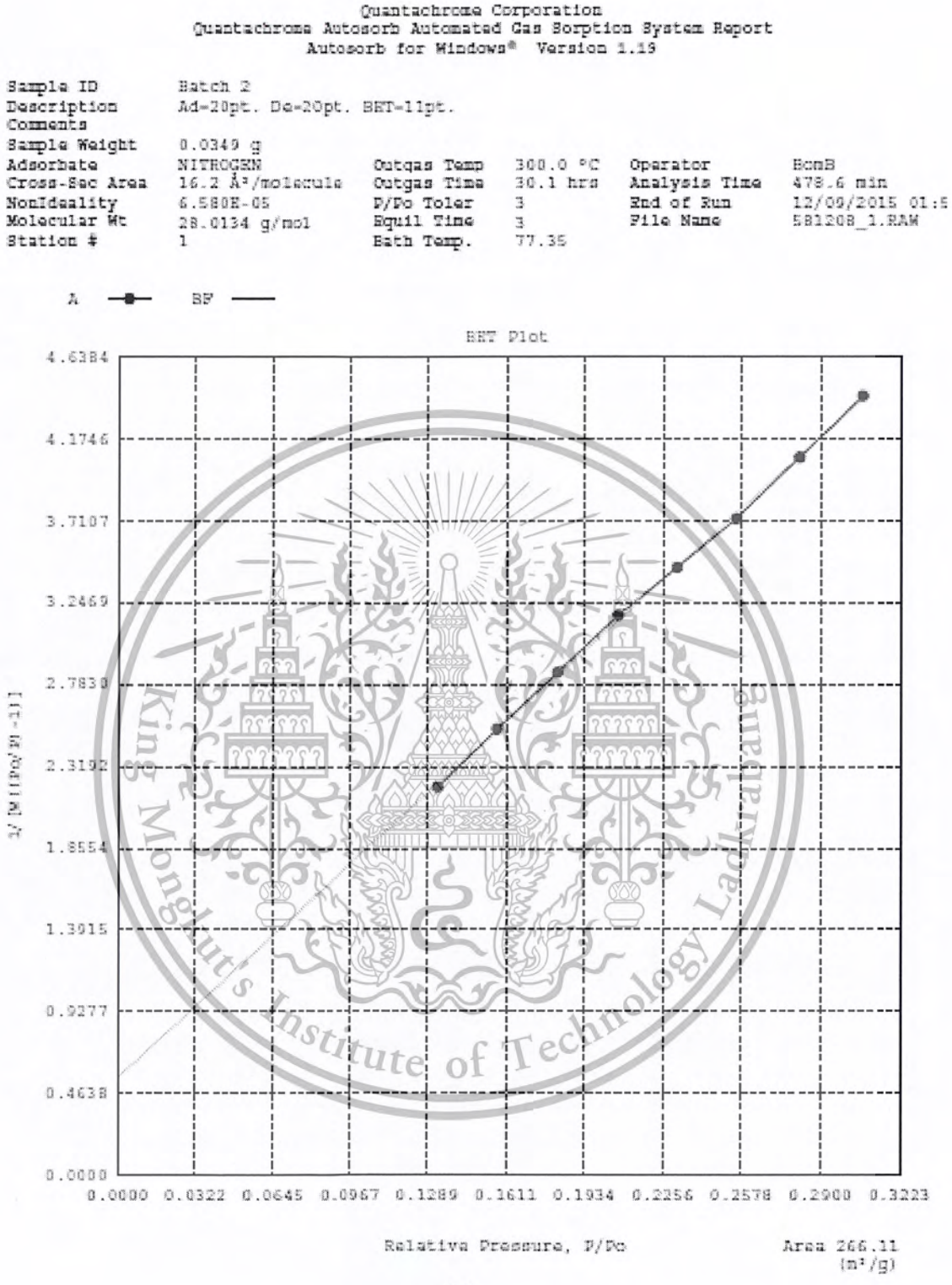

(b)

Figure A1 BET surface area plot of TNTs-HCl washed (a) and TNTs-DI water washed (b).

Quantachrome Corporation
Quantachrome Autosorb Automated Gas Sorption System Report
Autosorb for Windows® Version 1.19

Sample ID	H2 storage T batch1				
Description	Ads 22 Pts Des 22 Pts BET 11 pts				
Comments					
Sample Weight	0.0386 g				
Adsorbate	NITROGEN	Outgas Temp	300.0 °C	Operator	Nook
Cross-Sec Area	16.2 Å²/molecule	Outgas Time	23.9 hrs	Analysis Time	753.2 min
NonIdeality	6.580E-05	P/Po Toler	2	End of Run	08/26/2015
Molecular Wt	28.0134 g/mol	Equil Time	3	File Name	580825_2.RA
Station #	1	Bath Temp.	77.35		

MULTIPOINT BET

P/Po	Volume [cc/g] STP	1/[W((Po/P)-1)]
5.2659e-02	75.6396	5.880E-01
7.7284e-02	79.7725	8.401E-01
1.0280e-01	83.7368	1.095E+00
1.2790e-01	87.5324	1.341E+00
1.5304e-01	91.4264	1.581E+00
1.7799e-01	95.2303	1.819E+00
2.0248e-01	99.4054	2.044E+00
2.2727e-01	103.3668	2.277E+00
2.5192e-01	107.9139	2.497E+00
2.7631e-01	112.4440	2.717E+00
3.0153e-01	116.6686	2.961E+00

Area = 3.633E+02 m²/g

Slope = 8.471E+00

Y - Intercept = 1.163E-01

Correlation Coefficient = 0.999827

C = 8.285E+01

(a)

Quantachrome Corporation
Quantachrome Autosorb Automated Gas Sorption System Report
Autosorb for Windows® Version 1.19

Sample ID	Batch 2				
Description	Ad-20pt. De-20pt. BET-11pt.				
Comments					
Sample Weight	0.0349 g				
Adsorbate	NITROGEN	Outgas Temp	300.0 °C	Operator	BomB
Cross-Sec Area	16.2 Å²/molecule	Outgas Time	10.1 hrs	Analysis Time	478.6 min
NonIdeality	6.580E-05	P/Po Toler	3	End of Run	12/09/2015
Molecular Wt	28.0134 g/mol	Equil Time	3	File Name	581208_1.RA
Station #	1	Bath Temp.	77.35		

MULTIPOINT BET

P/Po	Volume [cc/g] STP	1/[W((Po/P)-1)]
1.3311e-01	55.7206	2.205E+00
1.5736e-01	59.0344	2.531E+00
1.8209e-01	62.4542	2.852E+00
2.0707e-01	65.7842	3.176E+00
2.3115e-01	69.8100	3.447E+00
2.5537e-01	73.6765	3.724E+00
2.8134e-01	76.9642	4.070E+00
3.0691e-01	80.2052	4.418E+00

Area = 2.661E+02 m²/g

Slope = 1.253E+01

Y - Intercept = 5.544E-01

Correlation Coefficient = 0.999674

C = 2.360E+01

(b)

Figure A2 Data of BET surface area of TNTs-HCl washed (a) and TNTs-DI water washed (b).

Quantachrome Corporation
Quantachrome Autosorb Automated Gas Sorption System Report
Autosorb for Windows® Version 1.19

Sample ID	H2 storage T batch1				
Description	Ads 22 Pts Des 22 Pts BET 11 pts				
Comments					
Sample Weight	0.0386 g				
Adsorbate	NITROGEN	Outgas Temp	300.0 °C	Operator	Nock
Cross-Sec Area	16.2 Å²/molecule	Outgas Time	23.9 hrs	Analysis Time	753.2 min
NonIdeality	6.580E-05	P/Po Toler	2	End of Run	08/26/2015 10:1
Molecular Wt	28.0134 g/mol	Equil Time	3	File Name	580825_2.RAW
Station #	1	Bath Temp.	77.35		

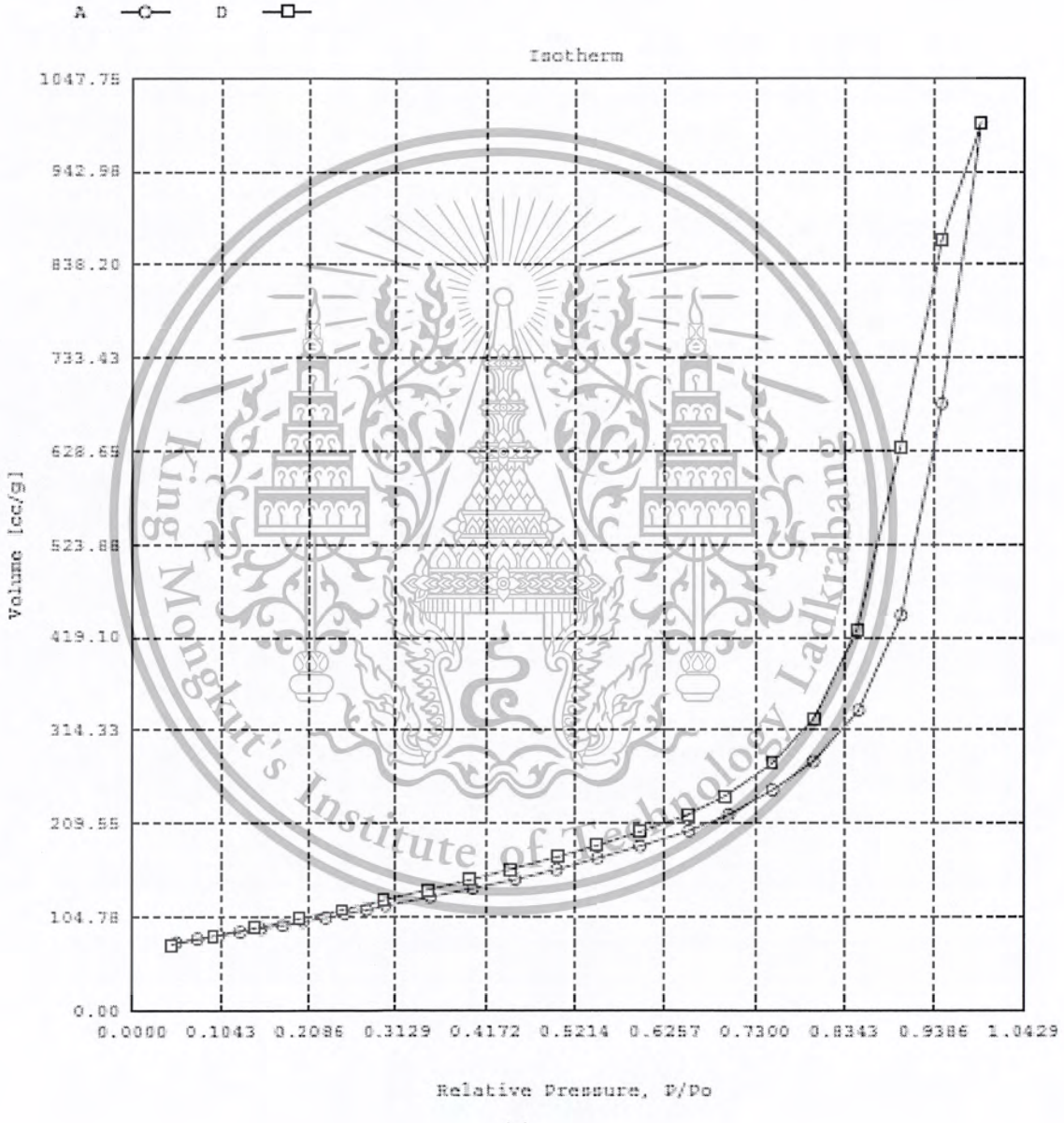

(a)

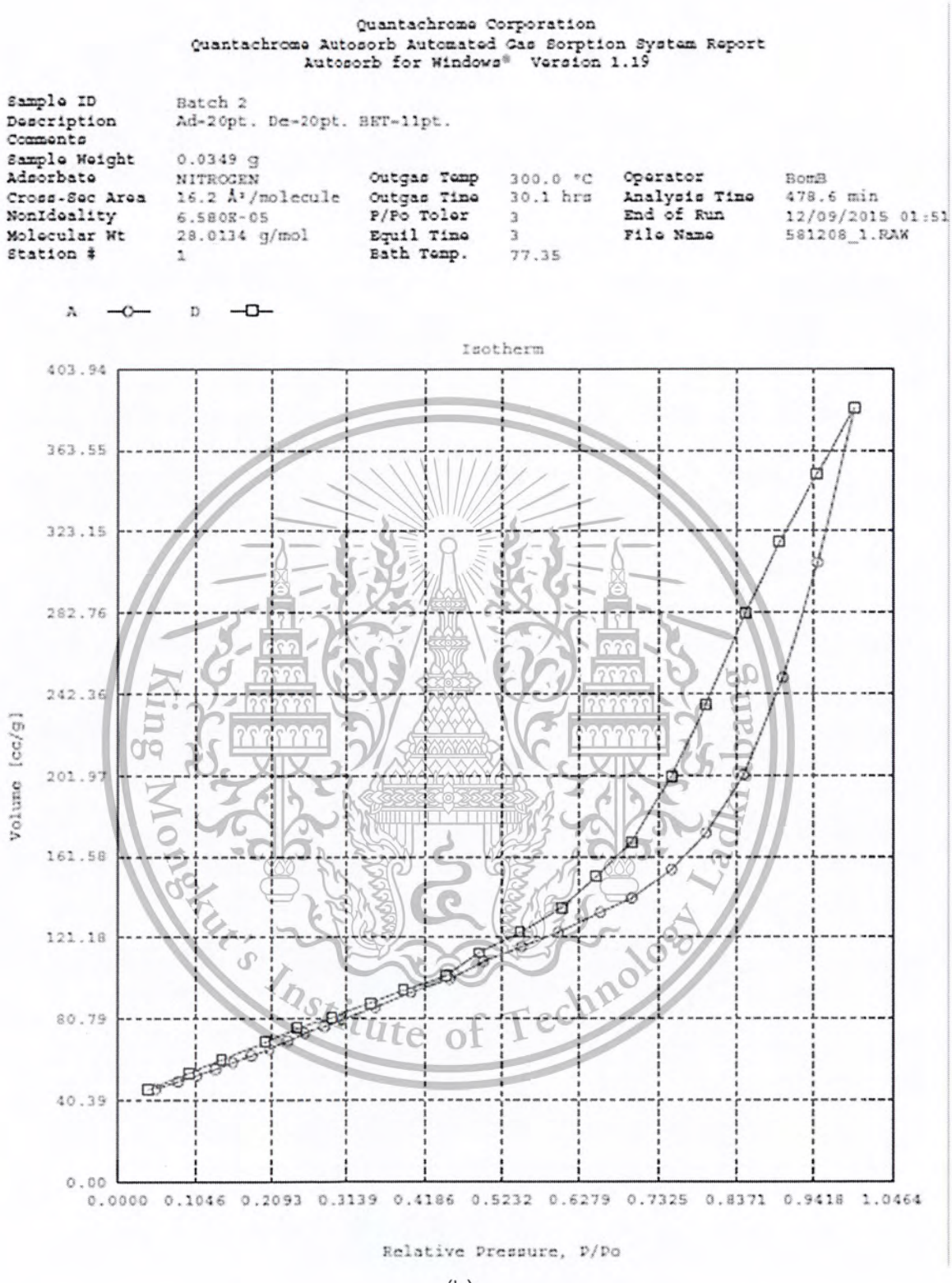

(b)

Figure A3 N_2 Adsorption-Desorption isotherm plot of TNTs-HCl washed (a) and TNTs-DI water washed (b).

Quantachrome Corporation
Quantachrome Autosorb Automated Gas Sorption System Report
Autosorb for Windows® Version 1.19

Sample ID	H2 storage T batch1				
Description	Ads 22 Pts Des 22 Pts BET 11 pts				
Comments					
Sample Weight	0.0386 g				
Adsorbate	NITROGEN	Outgas Temp	300.0 °C	Operator	Nook
Cross-Sec Area	16.2 Å²/molecule	Outgas Time	23.9 hrs	Analysis Time	753.2 min
NonIdeality	6.580E-05	P/Po Toler	2	End of Run	08/26/2015
Molecular Wt	28.0134 g/mol	Equil Time	3	File Name	580825_2.RA
Station #	1	Bath Temp.	77.35		

Isotherm

P/Po	Volume [cc/g] STP
5.2659e-02	75.6396
7.7284e-02	79.7725
1.0280e-01	83.7368
1.2790e-01	87.5324
1.5304e-01	91.4264
1.7799e-01	95.2303
2.0248e-01	99.4064
2.2727e-01	103.3668
2.5197e-01	107.9199
2.7631e-01	112.4440
3.0152e-01	116.6696
3.5414e-01	126.9702
4.0131e-01	136.6008
4.5251e-01	146.6075
5.0087e-01	157.6093
5.4910e-01	170.2109
5.9761e-01	183.7839
6.5428e-01	201.0870
6.9997e-01	218.2697
7.5039e-01	236.8186
7.9834e-01	258.9844
8.5105e-01	286.5311
9.0053e-01	318.7410
9.4072e-01	361.5751
9.9332e-01	427.8690
9.4766e-01	365.1739
8.9891e-01	331.2062
8.4927e-01	307.3705
7.9902e-01	287.3316
7.5020e-01	276.6321
6.9942e-01	260.2974
6.5277e-01	249.0598
5.9894e-01	240.2352
5.4776e-01	234.1723
5.0265e-01	232.1759
4.4594e-01	227.4845
3.9933e-01	226.0505
3.5017e-01	224.5008
2.9820e-01	223.2979
2.4797e-01	222.3246
1.9673e-01	222.3938
1.4546e-01	222.4339
9.5221e-02	223.0927

(a)

Quantachrome Corporation
Quantachrome Autosorb Automated Gas Sorption System Report
Autosorb for Windows® Version 1.19

Sample ID	Batch 2				
Description	Ad=20pt. De=20pt. BET=11pt.				
Comments					
Sample Weight	0.0349 g				
Adsorbate	NITROGEN	Outgas Temp	300.0 °C	Operator	BomB
Cross-Sec Area	16.2 Å²/molecule	Outgas Time	30.1 hrs	Analysis Time	478.6 min
NonIdeality	6.580E-05	P/Po Toler	3	End of Run	12/09/2015
Molecular Wt	28.0134 g/mol	Equil Time	3	File Name	581208_1.RA
Station #	1	Bath Temp.	77.35		

Isotherm

P/Po	Volume [cc/g] STP
5.2524e-02	46.0085
8.2541e-02	49.5645
1.0825e-01	52.6473
1.3311e-01	55.7206
1.5736e-01	59.0344
1.8209e-01	62.4542
2.0707e-01	66.7842
2.3119e-01	69.8100
2.5537e-01	73.6765
2.8134e-01	78.9642
3.0691e-01	80.2052
3.5213e-01	86.3603
4.0110e-01	93.9118
4.5035e-01	100.4567
4.9953e-01	109.3049
5.5054e-01	116.5201
6.0019e-01	123.7000
6.5451e-01	133.6536
6.9812e-01	140.7062
7.5114e-01	154.9102
7.9704e-01	171.0229
8.4757e-01	202.1444
9.0009e-01	250.2897
9.4711e-01	307.5072
9.9660e-01	384.7049
9.4662e-01	352.0197
8.9604e-01	317.9628
8.4972e-01	282.4968
7.9676e-01	237.2951
7.5068e-01	201.3146
6.9738e-01	168.4734
6.5109e-01	151.6504
6.0389e-01	135.8272
5.4781e-01	123.5544
4.9275e-01	113.5682
4.4702e-01	101.9106
3.9088e-01	94.7587
3.4678e-01	88.7261
2.9082e-01	81.2378
2.4454e-01	76.0865
2.0075e-01	69.0799
1.4105e-01	60.3436
9.6848e-02	53.9023

(b)

Figure A4 Data of N_2 Adsorption-Desorption isotherm of TNTs-HCl washed (a) and TNTs-DI water washed (b).

Quantachrome Corporation
Quantachrome Autosorb Automated Gas Sorption System Report
Autosorb for Windows® Version 1.19

Sample ID	H2 storage T batch1				
Description	Ads 22 Pts Des 22 Pts BET 11 pts				
Comments					
Sample Weight	0.0386 g				
Adsorbate	NITROGEN	Outgas Temp	300.0 °C	Operator	Nook
Cross-Sec Area	16.2 Å²/molecule	Outgas Time	23.9 hrs	Analysis Time	753.2 min
NonIdeality	6.5808-05	P/Po Toler	2	End of Run	08/26/2015 10:1
Molecular Wt	28.0134 g/mol	Equil Time	3	File Name	580825_2.RAW
Station #	1	Bath Temp.	77.35		

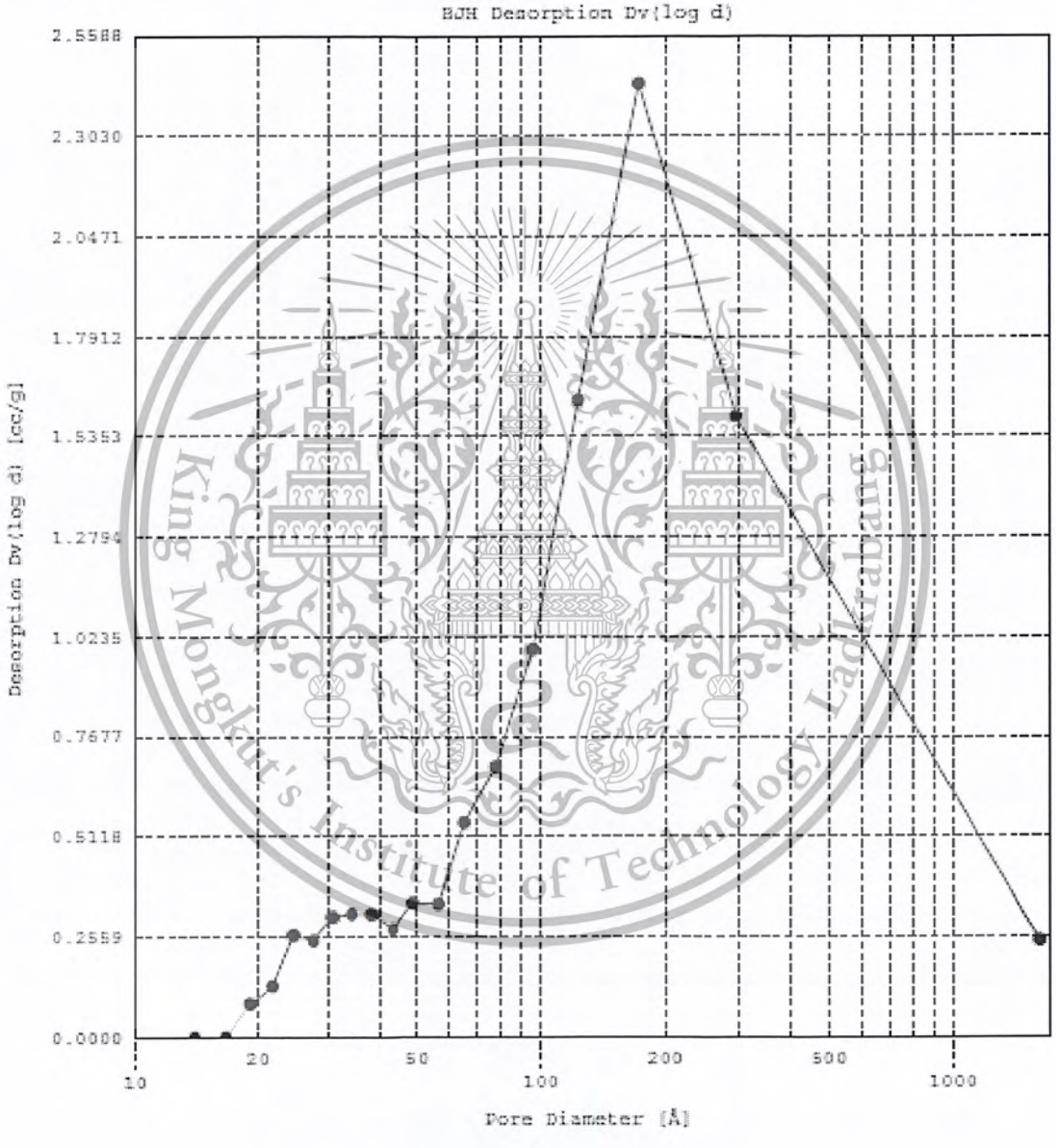

(a)

Quantachrome Corporation
Quantachrome Autosorb Automated Gas Sorption System Report
Autosorb for Windows® Version 1.19

Sample ID	Batch 2				
Description	Ad=20pt. De=20pt. BET=11pt.				
Comments					
Sample Weight	0.0349 g				
Adsorbate	NITROGEN	Outgas Temp	300.0 °C	Operator	BomB
Cross-Sec Area	16.2 Å²/molecule	Outgas Time	30.1 hrs	Analysis Time	478.6 min
NonIdeality	6.5808-05	P/Po Toler	3	End of Run	12/09/2015 01:5
Molecular Wt	28.0134 g/mol	Equil Time	3	File Name	581208_1.RAW
Station #	1	Bath Temp.	77.35		

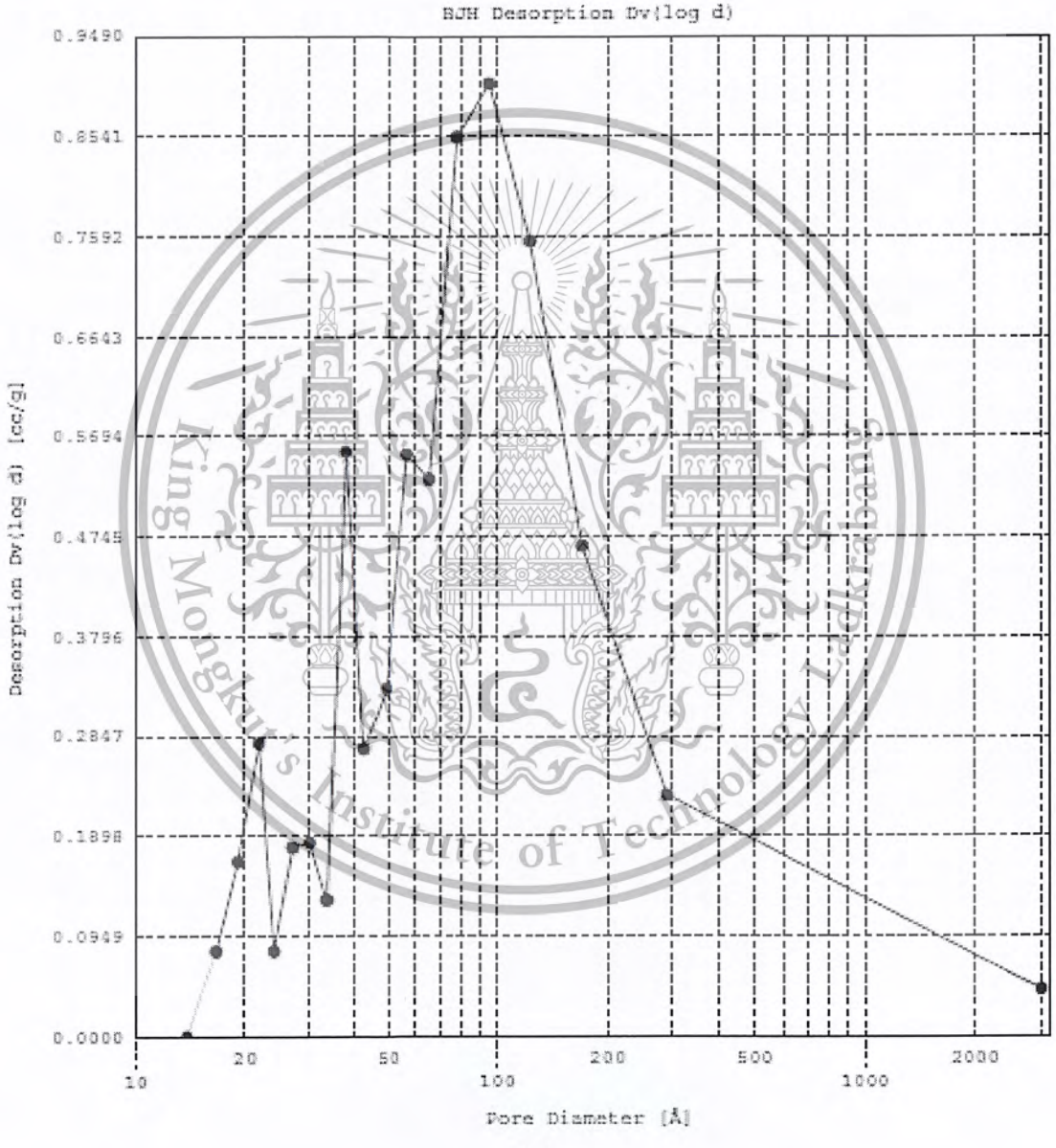

(b)

Figure A5 Pore size distribution plot of TNTs-HCl washed (a) and TNTs-DI water washed (b).

Quantachrome Corporation
Quantachrome Autosorb Automated Gas Sorption System Report
Autosorb for Windows® Version 1.19

Sample ID	H2 storage T batch1				
Description	Ads 22 Pts Des 22 Pts BET 11 pts				
Comments					
Sample Weight	0.0386 g				
Adsorbate	NITROGEN	Outgas Temp	300.0 °C	Operator	Nook
Cross-Sec Area	16.2 Å²/molecule	Outgas Time	23.9 hrs	Analysis Time	753.2 min
NonIdeality	6.580E-05	P/Po Toler	2	End of Run	08/26/2015
Molecular Wt	28.0134 g/mol	Equil Time	3	File Name	580825_2.RA
Station #	1	Bath Temp.	77.35		

BJH DESORPTION PORE SIZE DISTRIBUTION

Diameter Å	Pore Vol [cc/g]	Pore Surf Area [m²/g]	Dv(d) [cc/Å/g]	Ds(d) [m²/Å/g]	Dv(log d) [cc/g]	Ds(log d) [m²/g]
14.01	0.000E+00	0.000E+00	0.000E+00	0.000E+00	0.000E+00	0.000E+00
16.66	0.000E+00	0.000E+00	0.000E+00	0.000E+00	0.000E+00	0.000E+00
19.18	4.810E-03	1.003E+01	1.909E-03	3.981E+00	8.416E-02	1.755E+02
21.74	1.157E-02	2.247E+01	2.594E-03	4.772E+00	1.297E-01	2.386E+02
24.41	2.420E-02	4.317E+01	4.619E-03	7.569E+00	2.594E-01	4.250E+02
27.33	3.637E-02	6.097E+01	3.917E-03	5.732E+00	2.463E-01	3.604E+02
30.53	5.070E-02	7.975E+01	4.361E-03	5.714E+00	3.063E-01	4.013E+02
33.94	6.488E-02	9.646E+01	4.015E-03	4.732E+00	3.135E-01	3.694E+02
38.21	8.273E-02	1.151E+02	3.554E-03	3.720E+00	3.123E-01	3.268E+02
43.10	9.587E-02	1.273E+02	2.763E-03	2.564E+00	2.739E-01	2.542E+02
48.75	1.158E-01	1.437E+02	3.046E-03	2.499E+00	3.414E-01	2.801E+02
56.38	1.386E-01	1.598E+02	2.613E-03	1.854E+00	3.385E-01	2.402E+02
65.19	1.711E-01	1.796E+02	3.652E-03	2.241E+00	5.474E-01	3.359E+02
77.42	2.314E-01	2.110E+02	3.881E-03	2.005E+00	6.895E-01	3.562E+02
95.46	3.244E-01	2.499E+02	4.529E-03	1.897E+00	9.916E-01	4.155E+02
122.84	5.228E-01	3.145E+02	5.796E-03	1.887E+00	1.629E+00	5.303E+02
172.75	9.296E-01	4.087E+02	8.202E-03	1.436E+00	2.437E+00	5.643E+02
295.99	1.365E+00	4.675E+02	2.405E-03	3.250E-01	1.587E+00	2.144E+02
1615.09	1.578E+00	4.728E+02	8.685E-05	2.151E-03	2.462E-01	6.098E+00

(a)

Quantachrome Corporation
Quantachrome Autosorb Automated Gas Sorption System Report
Autosorb for Windows® Version 1.19

Sample ID	Batch 2				
Description	Ad=20pt. De=20pt. BET=11pt.				
Comments					
Sample Weight	0.0349 g				
Adsorbate	NITROGEN	Outgas Temp	300.0 °C	Operator	BomB
Cross-Sec Area	16.2 Å²/molecule	Outgas Time	30.1 hrs	Analysis Time	478.6 min
NonIdeality	6.580E-05	P/Po Toler	3	End of Run	12/09/2015
Molecular Wt	28.0134 g/mol	Equil Time	3	File Name	581208_1.RA
Station #	1	Bath Temp.	77.35		

BJH DESORPTION PORE SIZE DISTRIBUTION

Diameter Å	Pore Vol [cc/g]	Pore Surf Area [m²/g]	Dv(d) [cc/Å/g]	Ds(d) [m²/Å/g]	Dv(log d) [cc/g]	Ds(log d) [m²/g]
13.85	0.000E+00	0.000E+00	0.000E+00	0.000E+00	0.000E+00	0.000E+00
16.59	4.660E-03	1.123E+01	2.103E-03	5.069E+00	8.022E-02	1.934E+02
19.17	1.569E-02	3.425E+01	3.757E-03	7.840E+00	1.655E-01	3.454E+02
21.75	2.807E-02	5.701E+01	5.552E-03	1.021E+01	2.779E-01	5.110E+02
24.12	3.170E-02	6.303E+01	1.454E-03	2.411E+00	8.064E-02	1.338E+02
27.02	4.124E-02	7.715E+01	2.884E-03	4.269E+00	1.792E-01	2.653E+02
30.13	4.894E-02	8.738E+01	2.650E-03	3.519E+00	1.837E-01	2.439E+02
33.68	5.596E-02	9.572E+01	1.667E-03	1.980E+00	1.292E-01	1.534E+02
37.79	8.141E-02	1.227E+02	6.380E-03	6.754E+00	5.546E-01	5.871E+02
42.63	9.730E-02	1.376E+02	2.782E-03	2.610E+00	2.727E-01	2.559E+02
49.11	1.185E-01	1.548E+02	2.923E-03	2.381E+00	3.300E-01	2.688E+02
56.58	1.512E-01	1.779E+02	4.245E-03	3.001E+00	5.521E-01	3.903E+02
65.27	1.853E-01	1.988E+02	3.525E-03	2.160E+00	5.288E-01	3.241E+02
77.74	2.583E-01	2.364E+02	4.784E-03	2.462E+00	8.536E-01	4.392E+02
94.97	3.379E-01	2.699E+02	4.147E-03	1.747E+00	9.038E-01	3.807E+02
122.47	4.344E-01	3.014E+02	2.696E-03	8.806E-01	7.546E-01	2.465E+02
170.24	5.062E-01	3.183E+02	1.201E-03	2.821E-01	4.658E-01	1.094E+02
289.69	5.696E-01	3.271E+02	3.544E-04	4.893E-02	2.286E-01	3.157E+01
3016.58	6.212E-01	3.278E+02	9.783E-06	1.297E-04	4.398E-02	5.831E-01

(b)

Figure A6 Data of Pore size distribution of TNTs-HCl washed (a) and TNTs-DI water washed (b).

APENDIX B
GAS CHROMATOGRAM

Adsorption of carboxylic acid can be investigated by gas chromatography (GC), which can determine the amount of carboxylic acids (i.e. heptanoic and decanoic acid) left in the mother liquor/adsorbed onto TNTs.

Table B1 : The GC condition for the analysis of the adsorption profile of heptanoic acid onto TNTs washed with deionized water.

Column	DB-WAX (30 m x 0.25 mm x 0.25 μm)
Carrier gas	Nitrogen
Carrier gas flow rate	0.8 mL/min
Temperature program	40 °C hold 3 minute and go to 200 °C with rate 10 °C /min.
Split ratio	150

Table B2 : Summary of the peak area of heptanoic acid from the adsorption onto TNTs washed with deionized water at different adsorption time.

Time (h)	Area		Total area	Ratio heptanoic acid/isopropanol
	Isopropanol	Heptanoic acid		
0	57991	7252	65243	0.125053888
1	279689	27577	308387	0.098598801
2	32069	2486	34555	0.077520347
3	71146	4998	76144	0.070249909
4	60339	3934	64273	0.065198296
5	77384	4107	81491	0.053072987
6	74052	3416	77468	0.046129747
12	302182	13548	316770	0.044833908
36	48231	2147	69528	0.044514939

Calculation

$$\% \text{ Adsorption} = \frac{\text{(ratio acid/isopropanol) initial} - \text{(ratio acid/isopropanol) at time t}}{\text{(ratio acid/isopropanol) initial}} \times 100\%$$

% Adsorption (mass) : 1 g of TNTs, 75 mL of heptanoic acid

We used 10% w/w heptanoic acid in isopropanol

Assumed that d of the solution = 1 g/mL

Therefore, mass of acid in the starting liquid = 7.5 g

Total mol of heptanoic acid in the liquid : mol = g/MW

mol = 7.5/130.19

mol = 0.057608 mol or 57.608 mmol

Example

$$\% \text{ Adsorption} = \frac{\text{(ratio acid/isopropanol) 0 hr} - \text{(ratio acid/isopropanol) 1 hr}}{\text{(ratio acid/isopropanol) 0 hr}} \times 100\%$$

$$= \frac{0.125053888 - 0.098598801}{0.125053888} \times 100\%$$

$$= 21.15494962\ \%$$

$$\text{Mass adsorbed} = \frac{21.15494962 \times 7.5}{100} = 1.586621221 \text{ g}$$

$$\text{Adsorption (mmol)} = \frac{21.15494962 \times 57.608}{100} = 12.18694338 \text{ mmol}$$

Table B3 : The GC condition for the analysis of the adsorption profile of decanoic acid onto TNTs washed with deionized water.

Column	DB-WAX (30 m x 0.25 mm x 0.25 μm)
Carrier gas	Nitrogen
Carrier gas flow rate	0.8 mL/min
Oven temperature	40 °C hold 3 minute and go to 200 °C with rate 10 °C /min and hold at 200 °C 10 min.
Split ratio	150

Table B4 : Summary of the peak area of decanoicc acid from the adsorption onto TNTs washed with deionized water at different adsorption time.

Time (h)	Area		Total area	Ratio decanoic acid/Isopropanol
	Isopropanol	Decanoic acid		
0	213038	16796	229834	0.078840395
1	32853	1446	34299	0.044014245
2	128199	5320	133519	0.041497984
3	146458	5243	151701	0.035803328
4	151934	4660	156594	0.030671213
5	37963	890	38853	0.02344388
6	107527	1341	108868	0.012471286
12	59180	513	59693	0.008668469
36	109398	949	110347	0.008674747

Calculation

$$\% \text{ Adsorption} = \frac{(\text{ratio acid/isopropanol) initial} - (\text{ratio acid/isopropanol) at time t}}{(\text{ratio acid/isopropanol) initial}} \times 100\%$$

% Adsorption (mass) : 1 g of TNT used 75 mL of decanoic acid

We used 10% w/w decanoic acid in isopropanol

Assumed that d of the solution = 1 g/mL

Therefore, mass of acid in the starting liquid = 7.5 g

Total mol of the heptanoic acid in liquid: mol = g/MW

mol = 7.5/172.26

mol = 0.043539 mol or 43.539 mmol

Example

$$\% \text{ Adsorption} = \frac{(\text{ratio acid/isopropanol) 0 hr} - (\text{ratio acid/isopropanol) 1 hr}}{\text{ratio acid/isopropanol 0 hr}} \times 100\%$$

$$= \frac{0.078840395 - 0.044014245}{0.078840395} \times 100\%$$

$$= 44.17297757\ \%$$

$$\text{Mass adsorbed} = \frac{44.17297757 \times 7.5}{100} = 3.312973318\ \text{g}$$

$$\text{Adsorption (mmol)} = \frac{44.17297757 \times 43.539}{100} = 19.23247245\ \text{mmol}$$

APPENDIX C

ATR SPECTRA OF ALKALI TITANTES PRIOR TO THE ADSORPTION

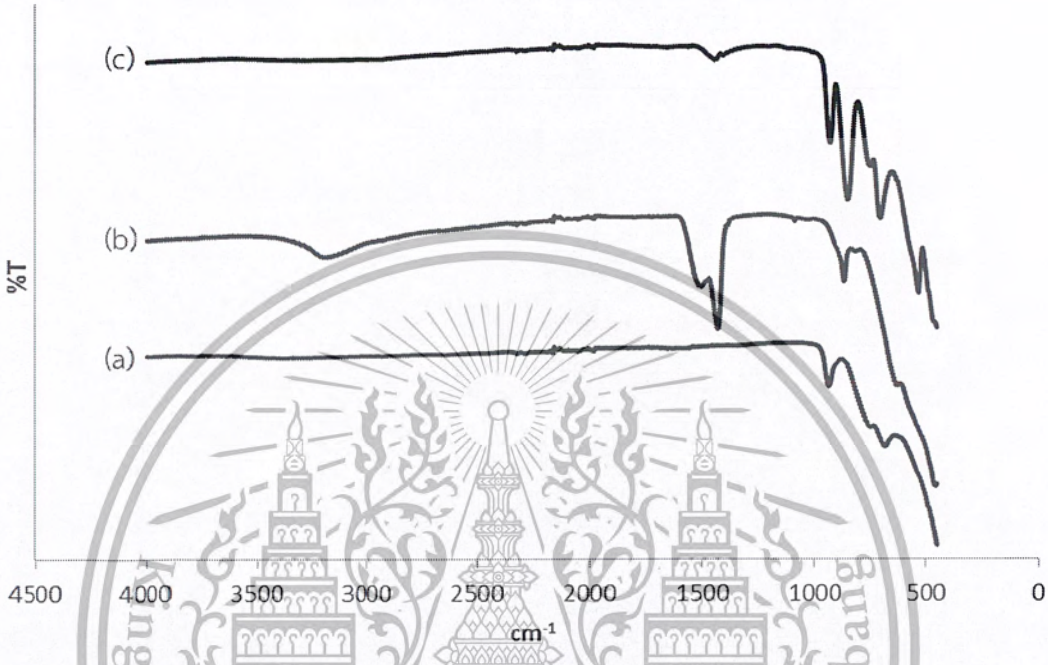

Figure C1 ATR spectra of the alkali titanates prior to the adsorption: $K_2Ti_6O_{13}$ (a), Li_2TiO_3 (b) and $Na_2Ti_3O_7$ (c).

APPENDIX D

ANALYSIS AFTER THE ADSORPTION TO TNTs AND KZn MICROCRYSTALS

THERMOGRAVIMATIC ANALYSIS

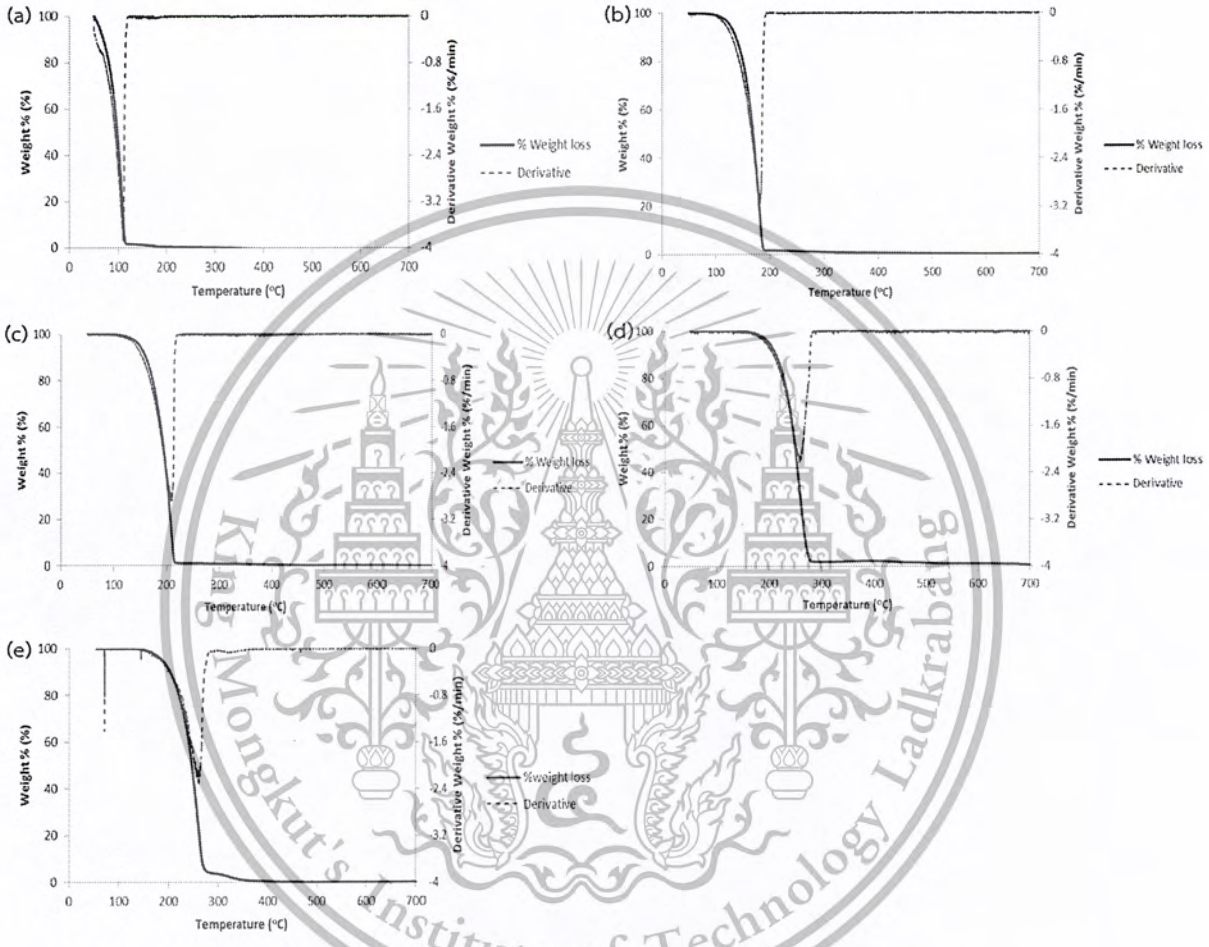

*Test condition; in nitrogen from 50 to 700°C (10°C/min)

Figure D1 Mass loss curve of pure carboxylic acid ; propanoic acid (a), heptanoic acid (b), decanoic acid (c), sebacic acid (d) and palmitic acid (e).

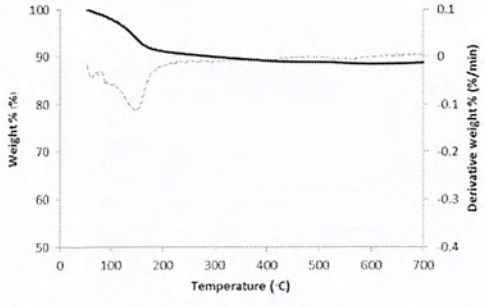

Figure D2 Mass loss curve of TNTs refluxed with isopropanol.

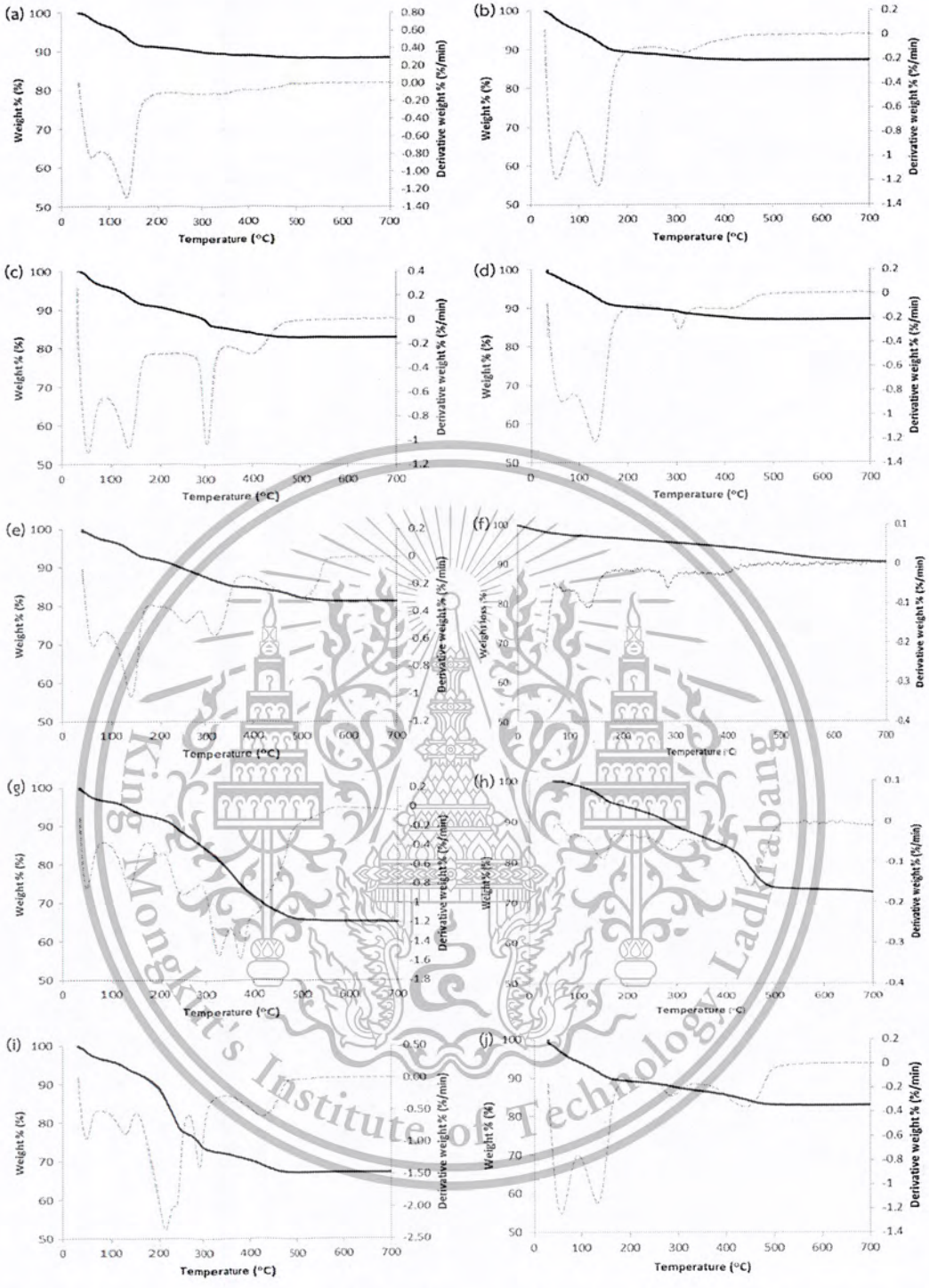

Figure D3 Mass loss curves of TNTs refluxed with carboxylic acid; TNTs+propanoic acid non-washed (a), TNTs+propanoic acid washed (b), TNTs+heptanoic acid non-washed (c), TNTs+heptanoic acid washed (d), TNTs+decanoic acid non-washed (e), TNTs+decanoic acid washed (f), TNTs+sebacic acid non-washed (g), TNTs+sebacic acid washed (h), TNTs+palmitic acid non-washed (i), TNTs+palmitic acid washed (j).

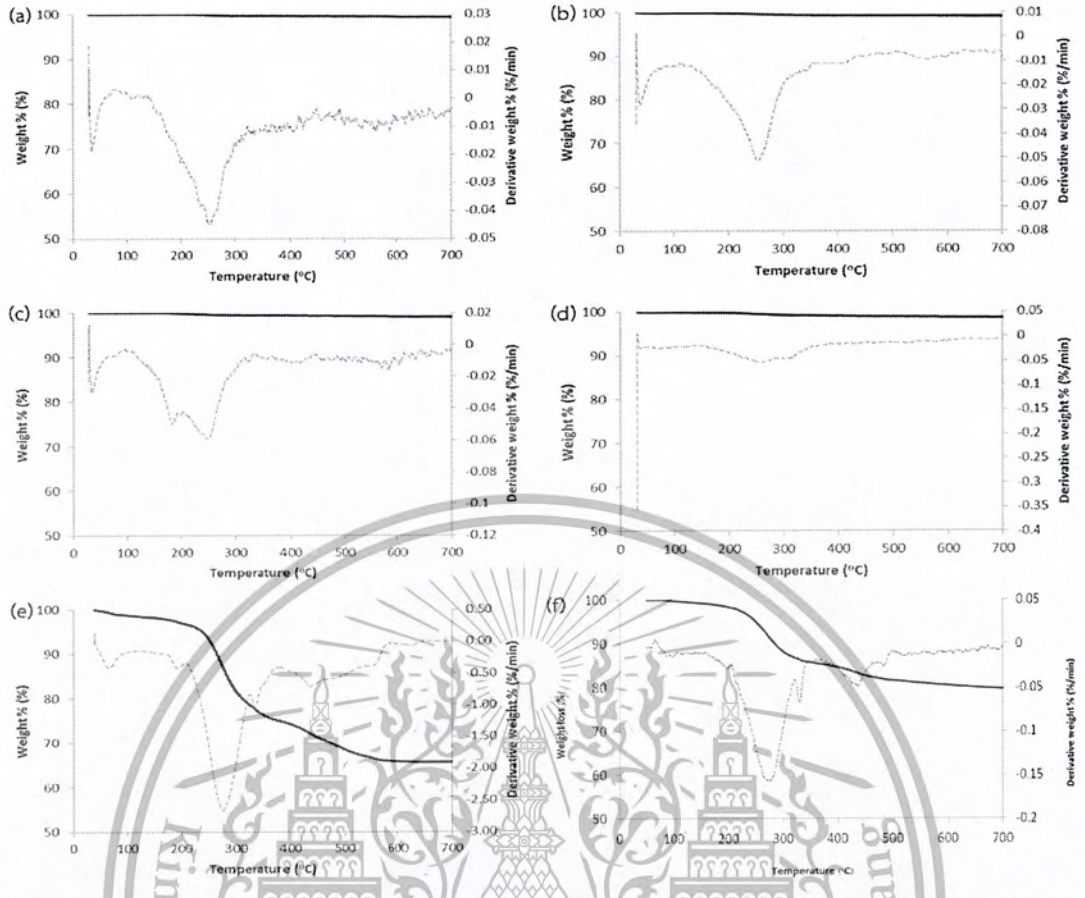

Figure D4 Mass loss curve of lepidocrocite titanate microcrystals ($K_{0.8}Zn_{0.4}Ti_{1.6}O_4$, KZn) refluxed with carboxylic acid: KZn+propanoic acid non-washed (a), KZn+propanoic acid washed (b), KZn+heptanoic acid non-washed (c), KZn+heptanoic acid washed (d), KZn+sabacic acid non-washed (e), KZn+sabacic acid washed (f).

Table D1 % Mass loss and decomposition temperature of pure carboxylic acids and the materials after the adsorption of carboxylic acids.

Sample	% Mass loss and Temperature part 1	% Mass loss and Temperature part 2	% Mass loss and Temperature part 3	Total mass loss
Propanoic acid	100.0% 100 °C	-	-	100.0%
Heptanoic acid	100.0% 171 °C	-	-	100.0%
Decanaic acid	100.0% 206 °C	-	-	100.0%
Sebacic acid	100.0% 260 °C	-	-	100.0%
Palmitic acid	100.0% 261 °C	-	-	100.0%
TNTs+isopropanol (Blank)	9.6% 131 °C	-	-	9.6%
TNTs+propanoic acid non-washed	9.2% 62-134 °C	1.8% 334 °C	0.6% 426 °C	11.6%
TNTs+propanoic acid washed	11.1% 54-141 °C	1.7% 315 °C	-	12.8%
TNTs+heptanoic acid non-washed	10.0% 52-138 °C	4.9% 304 °C	2.2% 398 °C	17.1%
TNTs+heptanoic acid washed	9.8% 64-133 °C	1.9% 306 °C	1.2% 408 °C	12.9%
TNTs+decanoic acid non-washed	7.5% 64-143 °C	7.5% 258-318 °C	3.6% 493 °C	18.6%
TNTs+decanoic acid washed	9.2% 125 °C	2.3% 274 °C	1.9% 378 °C	13.4%
TNTs+sebacic acid non-washed	7.2% 46-136 °C	14.6% 252-324 °C	12.9% 373 °C	34.7%
TNTs+sebacic acid washed	3.8% 135 °C	3.6% 280 °C	10.0% 441 °C	17.4%
TNTs+palmitic acid non-washed	6.8% 45-129 °C	21.0% 213-290 °C	4.9% 426 °C	32.7%

Sample	% Mass loss and Temperature part 1	% Mass loss and Temperature part 2	% Mass loss and Temperature part 3	Total mass loss
TNTs+palmitic acid washed	10.7% 55-132 °C	2.3% 284 °C	3.8% 438 °C	16.8%
KZn+propanoic acid non-washed	-	0.7% 252 °C	-	0.7%
KZn+propanoic acid washed	-	1.0% 255 °C	-	1.0%
KZn+heptanoic acid non-washed	-	2.7% 247 °C	-	2.7%
KZn+heptanoic acid washed	-	1.4% 261 °C	-	1.4%
KZn+sebacic acid non-washed	1.7% 66 °C	23.3% 277 °C	9.4% 439 °C	34.4%
KZn+sebacic acid washed	-	13.2% 261 °C	2.7% 422 °C	15.9%

APENDIX E
BASICITY

Example E1 : Calculation of Sanderson intermediate electronegativity and partial negative charges of framework oxygen of Li_2TiO_3

Table E1 : Electronegativity and total composition per one Ti atom.

Element	Li	Ti	O
Electronegativity from relative atomic compactness	0.74	1.40	5.21
Total composition per one Ti atom of Li_2TiO_3	2.00	1.00	3.00

Sanderson intermediate electronegativity

$$S_{int} = [\prod iSi^{Pi}]^{\frac{1}{\sum iPi}}$$

$$S_{int} = [(0.74^{2})(1.40^{1})(5.21^{3})]^{1/6}$$

$$= 2.1837$$

$$\sigma_1 = \frac{S_{int} - S_i}{2.08\,(S_i)^{1/2}}$$

$$\sigma_1 = \frac{2.1837 - 5.21}{2.08\,(5.21)^{1/2}}$$

$$\sigma_1 = -0.6374$$

Table E2 : Partial negative charges of framework oxygen (σ_1) of materials

Materials	Partial negative charges of framework oxygen (σ_1)
Li_2TiO_3	-0.6374
$Na_2Ti_3O_7$	-0.5319
TNTs	N/A
$K_{0.8}Zn_{0.4}Ti_{1.6}O_4$	-0.5175
$K_2Ti_6O_{13}$	-0.5042

Table E3 : Electronegativity from relative atomic compactness.

Element	Electronegativity from relative atomic compactness*
Ti	1.40
O	5.21
Li	0.74
Na	0.70
K	0.42
Zn	3.00
H	3.55

*From literature [32].